3-1969

Electrochemical Measurements in Molten Fluorides

Howard W. Jenkins
University of Tennessee - Knoxville

To the Graduate Council:

I am submitting herewith a dissertation written by Howard W. Jenkins entitled "Electrochemical Measurements in Molten Fluorides." I have examined the final electronic copy of this dissertation for form and content and recommend that it be accepted in partial fulfillment of the requirements for the degree of Doctor of Philosophy, with a major in Chemistry.

Gleb Mamantov, Major Professor

We have read this dissertation and recommend its acceptance:

William Bull, Henry P. Carer, G. P. Smith

Accepted for the Council:

Carolyn R. Hodges

Vice Provost and Dean of the Graduate School

(Original signatures are on file with official student records.)

February 28, 1969

To the Graduate Council:

I am submitting herewith a dissertation written by Howard W. Jenkins, Jr., entitled "Electrochemical Measurements in Molten Fluorides." I recommend that it be accepted in partial fulfillment of the requirements for the degree of Doctor of Philosophy, with a major in Chemistry.

Gleb Mamantov
Major Professor

We have read this dissertation
and recommend its acceptance:

William E Bell

James C White

Harvey P. Carter

G. P. Smith

Accepted for the Council:

Hilton A. Smith
Vice Chancellor for
Graduate Studies and Research

ELECTROCHEMICAL MEASUREMENTS IN MOLTEN FLUORIDES

A Dissertation

Presented to

the Graduate Council of

The University of Tennessee

In Partial Fulfillment

of the Requirements for the Degree

Doctor of Philosophy

---

by

Howard W. Jenkins, Jr.

March 1969

To my parents and wife for their encouragement, love and understanding.

ACKNOWLEDGEMENT

The author wishes to express his thanks to the following people and organizations: Professor Gleb Mamantov for his advice and direction, D. L. Manning for his valuable assistance and suggestions in the laboratory, J. P. Young for spectrophotometric analysis of molten salt samples containing uranium, the Chemistry Department of the University of Tennessee for providing financial support during a portion of my studies in the form of a teaching assistantship, the Atomic Energy Commission for financial support in the form of a research assistantship on Contract AT-(40-1)-3518, Oak Ridge Associated Universities for financial support in the form of a fellowship, the General Analysis Laboratories of the Analytical Chemistry Division, the Oak Ridge National Laboratory for analysis of samples, and the Oak Ridge National Laboratory operated for the United States Atomic Energy Commission by Union Carbide Corporation, especially the Analytical Chemistry Division, for providing the equipment, materials and facilities for this research.

ABSTRACT

The nickel(II)/nickel couple, contained in a boron nitride compartment, was shown to be a useful reference electrode in fluoride melts. From emf measurements on nickel(II)/nickel concentration cells, the nickel(II)/nickel couple was shown to obey the Nernst equation in molten LiF-NaF-KF (46.5-11.5-42.0 mole per cent) and LiF-BeF_2-ZrF_4 (65.6-29.4-5.0 mole per cent). It was found that in some cases the reference electrode had a significant junction potential across the boron nitride wall.

Kinetics of the charge transfer reaction Ni(II) + 2e = Ni were investigated by the voltage-step method. Apparent adsorption of nickel(II) at the microelectrode surface complicated the interpretation of the data.

Employing the nickel(II)/nickel reference electrode as one half-cell, several standard electrode potentials were determined from emf measurements on galvanic cells. The standard electrode potential of the nickel(II)/nickel couple was arbitrarily set at 0.000 V. The following values were determined in LiF-BeF_2-ZrF_4 at 500°: beryllium(II)/beryllium, -2.120 V; zirconium(IV)/zirconium, -1.742 V; uranium(IV)/uranium(III), -1.480 V; chromium(II)/chromium, -0.701 V; chromium(III)/chromium(II), -0.514 V; iron(II)/iron, -0.410 V; nickel(II)/nickel, 0.000 V; iron(III)/iron(II), 0.166 V. The following values were determined in LiF-NaF-KF at 500°: iron(II)/iron, -0.390 V; iron(III)/iron(II), -0.200 V; nickel(II)/nickel, 0.000 V.

A simple voltammetric method was developed for the determination of high U(IV)/U(III) ratios. The method involves the measurement of the equilibrium potential of the melt with respect to the voltammetric equivalent of the standard electrode potential, the polarographic $E_{1/2}$, of the uranium(IV)/uranium(III) couple.

TABLE OF CONTENTS

LIST OF TABLES

LIST OF FIGURES

FIGURE PAGE

CHAPTER I

INTRODUCTION

Electrode potentials give a direct measure of the thermodynamic stability of electroactive species relative to one another in a given solvent and provide information useful in electroanalytical chemistry. This dissertation deals with electrochemical measurements in molten fluorides. Interest in molten fluorides stems from their importance in nuclear reactor technology, production of aluminum and fluorine, and the electrodeposition of refractory metals. Only a small number of electrode potentials have been measured in molten fluorides when compared to the large amount of data available in molten chlorides. Summaries of electrode potentials in molten salt solvents are available in recent reviews.[1-3]

The work of Laitinen and Liu[4] represents the determination of a rather comprehensive emf series in a molten salt solvent, in this case a LiCl-KCl eutectic at 450°. Concentrations of the soluble electrode species were varied from about 0.001 to 0.5 molar in the bulk of the melt, and the cell emf's were measured versus a 0.01 to 0.1 molar platinum(II)/platinum reference electrode contained in a glass tube with a fritted bottom. Standard (or formal) electrode potentials were obtained by extrapolating the cell emf's by means of the Nernst equation to the hypothetical one molar solutions for both the reference electrode and the indicator electrode. In reporting the electrode potentials, the potential of a one molar platinum(II)/platinum reference electrode was

arbitrarily set at 0.00 V. A similar investigation in molten fluorides should provide much useful information.

A. REVIEW OF THE LITERATURE

1. Reference Electrodes in Molten Fluorides

A reference electrode is required for the measurement of electrode potentials. Such an electrode should be stable and reproducible. The incompatibility of many common materials (for example, glass, quartz and alumina) with the fluoride environment has presented experimenters with many difficulties in the design of a practical reference electrode. Reviews are available on reference electrodes in molten salts including fluorides.[1,3,5]

Since chlorine/chloride, bromine/bromide and iodine/iodide reference electrodes have been used successfully in their respective melts,[6] it might be expected that the fluorine/fluoride couple could be developed into a reference electrode in fluoride melts. Simons and Hildebrand[7] attempted to use such an electrode in molten potassium hydrogen fluoride. A graphite rod immersed in the melt was anodized to saturate it and the melt with fluorine; however, on cessation of electrolysis, the potential decreased rapidly. Under similar conditions, Arvia and deCusminsky[8,9] have obtained a reproducible emf of 1.75 V for the cell C/F_2, $HF_2^-//HF$, H_2/Cu in potassium hydrogen fluoride at 250°; this emf was stable for at least several minutes.

Dirian, Romberger and Baes[10] have shown the reversibility of a hydrogen fluoride/hydrogen electrode in molten $LiF-BeF_2$ (66-34 mole per cent), and Hitch and Baes[11] have employed a similar reference electrode

in the determination of beryllium(II) activity in LiF-BeF_2 mixtures. The electrode consisted of a palladium tube immersed in the melt and bathed with a hydrogen fluoride-hydrogen mixture. A boron nitride or graphite compartment separated the electrode from the bulk of the melt. Ionic contact was made through a 3/32 in. hole in the bottom of the compartment. The potential of the electrode responded to changes in the partial pressures of hydrogen and hydrogen fluoride as predicted by the Nernst equation. Difficulties involved with handling gas electrodes at high temperatures make the fluorine/fluoride and hydrogen fluoride/hydrogen couples undesirable as practical reference electrodes.

A two compartment silver chloride/silver reference electrode was designed by Coriou, Dirian and Hure[12] for use in molten fluorides. The inner compartment consisted of a quartz tube closed at the bottom with a zirconium oxide-asbestos cement plug; it contained a silver wire immersed in molten silver chloride. The outer compartment was a graphite tube with a threaded graphite plug at the bottom; it contained the inner compartment immersed in sodium chloride. Ionic contact between the two compartments was provided by the zirconium oxide-asbestos plug. Fused salt that penetrated the threads of the graphite plug provided ionic contact between the outer compartment and the bulk of the melt. Disadvantages of this electrode are complexity of design and probable inclusion of two significant junction potentials in the measured emf.

Winand and Chaudron[13] have also employed a silver chloride/silver electrode in a fluoride melt. In this case a boron nitride compartment with a sodium borate plug in the side, to provide ionic contact with the bulk of the melt, contained a silver wire immersed in a AgCl-NaCl mixture.

In light of the present work, the use of the sodium borate plug appears unnecessary to provide ionic contact between the half-cells.

Pizzini and Morlotti[14] have employed a solid galvanic half-cell, nickel oxide/nickel, as an external reference electrode for overvoltage measurements in LiF-NaF-KF (46.5-11.5-42.0 mole per cent) at 600°. A sintered wall of zirconium oxide doped with calcium oxide, an ionic conductor at high temperatures, provided the necessary ionic contact between the reference half-cell and the bulk of the melt. Overvoltage measurements were made versus a platinum or nickel wire probe immersed in the melt; the potential of the probe was measured with respect to the reference electrode by means of a high impedance measuring device. Apparently the reference electrode was so easily polarized that direct measurement of potentials with respect to it was not possible.

Emf measurements in molten NaF-KF (40-60 mole per cent) at 850° were made by Grjotheim[15] employing a nickel(II)/nickel reference electrode. The electrode consisted of a nickel wire immersed in a solution of nickel fluoride in the solvent salt and contained in a platinum crucible. Ionic contact with the bulk of the melt was made by means of a sintered alumina salt bridge connecting the two half-cells. The salt bridge was prepared by dipping the sintered alumina rod into an aqueous solution of the solvent salt and drying it before use. The rod was readily attacked by the fluoride melt; therefore, it was mounted so that it could be removed from the melt when measurements were not being made. Senderoff, Mellors and Reinhart[16] have used a nickel(II)/nickel reference electrode, very similar to that employed by Grjotheim, for chronopotentiometric measurements in molten LiF-NaF-KF (46.5-11.5-42.0 mole per cent). On long contact with

the melt, corrosion of the alumina bridge introduced impurities, thought to be iron and aluminum, into the melt.

2. Electrode Potentials in Molten Fluorides

Table I summarizes the data presently available from measurements, estimates and calculations of electrode potentials in molten fluoride solvents for cation electrodes, the hydrogen fluoride/hydrogen electrode and the fluorine/fluoride electrode. For the sake of comparison, all the values cited in Table I are given with respect to the nickel(II)/nickel electrode. The results cited in Table I are discussed briefly below.

Only two groups have obtained emf data from measurements on galvanic cells. Grjotheim[15] has measured the potentials of several metal ion/metal electrodes in NaF-KF (40-60 mole per cent) at 850° (see column I of Table I). However, questions have been raised regarding the oxidation states of the chromium and iron ions in these measurements. Mellors and Senderoff[17] believe that the electrode couples were chromium(III)/chromium(II) and iron(III)/iron(II) rather than chromium(III)/chromium and iron(III)/iron as indicated by Grjotheim. Hitch and Baes[11] have measured the potential of a beryllium(II)/beryllium electrode versus a hydrogen fluoride/hydrogen electrode in LiF-BeF_2 (66-34 mole per cent).

Mellors and Senderoff[17] have estimated the potentials of several redox couples from chronopotentiograms obtained at solid indicator electrodes in NaF-KF-LiF (46.5-11.5-42.0 mole per cent) at 750°. The potentials were measured at one fourth of the transition time, $E_{\tau/4}$; this potential is approximately the standard potential of the electrode reaction. These values are given in column II of Table I with respect to a hypothetical unit mole fraction nickel(II)/nickel reference electrode.

TABLE I

ELECTRODE POTENTIALS IN MOLTEN FLUORIDES

Redox couple	I[a]	II[b]	III[c]	IV[d]	V[e]	VI[f]
Li(I)/Li			-0.62[g]	-3.012	-2.29	-2.674
Ba(II)/Ba					-2.17	-2.657
La(III)/La				-2.68	-1.85	-2.518
Ce(III)/Ce				-2.61	-1.86	-2.445
Sm(III)/Sm				-2.48		-2.323
Na(I)/Na			-1.18[g]			-2.229
K(I)/K			-0.96[g]			-2.127
Th(IV)/Th				-2.332	-1.95	-1.675
Be(II)/Be				-2.211	-2.22	-1.517
Zr(IV)/Zr				-1.772		-1.352
U(III)/U				-1.838		
U(IV)/U				-1.752	-1.7	-1.327
U(IV)/U(III)				-1.517		
Al(III)/Al	-1.5	-1.7	-0.67			-0.977
Ta(II)/Ta		-1.46				
Mn(II)/Mn	-1.04		-0.66			-0.680
Cr(II)/Cr		-1.33		-0.789		-0.510
Ta(V)/Ta(II)		-1.23				
Nb(I)/Nb		-1.23				
Nb(IV)/Nb(I)		-0.957				
Cr(III)/Cr	-0.70					-0.377
Cr(III)/Cr(II)		-0.89	0.72			
Zn(II)/Zn			-0.58			-0.375
Fe(II)/Fe		-0.715		-0.413		-0.204
HF/1/2H_2				-0.285		
Cd(II)/Cd			-0.40			-0.145
Nb(V)/Nb(IV)		-0.31				
Co(II)/Co	-0.07		-0.14			-0.032
Ni(II)/Ni	0.00	0.00	0.00	0.00	0.00	0.000
Pb(II)/Pb			-0.16			0.025
Fe(III)/Fe	-0.12					0.058
Fe(III)/Fe(II)		-0.41	0.58			
Cu(I)/Cu	0.48					
Bi(III)/Bi			0.22			0.348
Cu(II)/Cu						0.684
Ag(I)/Ag	0.64					1.216
1/2F_2/F^-			1.58	2.129		2.890

TABLE I (CONTINUED)

[a]In NaF-KF (40-60 mole per cent) at 850° (K. Grjotheim, Z. Physik. Chem., N. F. 11, 150 (1957)).

[b]In LiF-NaF-KF (46.5-11.5-42.0 mole per cent) at 750° (G. W. Mellors and S. Senderoff in "Applications of Fundamental Thermodynamics to Metallurgical Processes," G. R. Fitterer, Ed., Gordon and Breach, New York, N. Y., 1967, pp. 81-103).

[c]For five mole percent solutions in NaF at 1000° (Yu. K. Delimarskii and F. F. Grigorenko, Ukr. Khim. Zh., 22, 726 (1956)).

[d]In LiF-BeF_2 (66-34 mole per cent) at 500° (C. F. Baes, Jr., in SM-66/60, "Thermodynamics," Vol. I, IAEA, Vienna, 1966).

[e]In LiF-BeF_2 (66-34 mole per cent) at 600° (D. M. Moulton, W. F. Teichert, W. K. R. Finnell, W. R. Grimes and J. H. Shaffer, U.S.A.E.C. Report ORNL - 4229, 39 (1968)).

[f]For solid fluorides at 500° (W. J. Hamer, M. S. Malmberg and R. Rubin, J. Electrochem. Soc., 112, 750 (1965)).

[g]For pure fluorides at 1000° (Yu. K. Delimarskii and F. F. Grigorenko, Ukr. Khim. Zh., 22, 726 (1956)).

Electrode potentials may be estimated from the relative decomposition potentials of electrode couples in a common solvent. Delimarskii and Grigorenko[18] have reported decomposition potentials for pure sodium fluoride, potassium fluoride, lithium fluoride and a number of five mole per cent solutions of metal fluorides in sodium fluoride at 1000°. The values given in column III of Table I are with respect to the decomposition potential of the five mole per cent nickel fluoride solution. The values of the alkali metal fluorides are also included even though the solvent effect is not the same. The decomposition potential values appear to be too low when compared with estimates from free energies of formation.[21] This general result was probably due to an anode reaction other than the oxidation of the fluoride ion, such as the oxidation of the oxide ion or the graphite (to form a CF_x type product). Even if the anode reaction was not the oxidation of the fluoride ion, only the potential assigned to the fluorine/fluoride electrode would be in error if the anode reactions were the same in all experiments. In several instances, the trend in electrode potentials determined by this method differs significantly from that generally observed in Table I; therefore, it appears that the potential of the anode reaction varied significantly between experiments.

Baes[19] has calculated the potentials of several electrode couples from thermodynamic data available for various ions in LiF-BeF_2 (66-34 mole per cent). These values at 500° are given in column IV of Table I along with the values of the beryllium (II)/beryllium and hydrogen fluoride/hydrogen electrodes measured by Hitch and Baes.[11] The standard states for the lithium, berryllium and fluoride ions are determined by the solvent composition, and the standard states for the other solutes are the hypothetical unit mole fraction solutions.

Moulton, Teichert, Finnell, Grimes and Shaffer[20] have also calculated several electrode potentials in LiF-BeF_2 (66-34 mole per cent). Calculations were based upon distribution equilibria data between the melt and liquid bismuth. Since the potential of nickel(II)/nickel couple was not calculated, the electrode potentials given in column V of Table I are related to the potential of a hypothetical unit mole fraction nickel(II)/nickel reference electrode by the beryllium(II)/beryllium potential value given by Baes.[19] The standard states of lithium and beryllium ions are determined by the solvent composition while the standard states of the other solutes and metals (in liquid bismuth, except for beryllium metal) are the hypothetical unit mole fraction solutions.

For the sake of comparison, theoretical electrode potentials for solid fluorides at 500° are given in column VI of Table I.[21] These values were calculated for cells containing a single fluoride salt from free energies of formation; interactions between components were not considered.

3. Electrode Kinetics of the Nickel(II)/Nickel Couple in Molten Salts

Charge transfer rate constants have been shown to be generally fast in molten salts.[22] The a.c. impedance method and the relaxation methods have been used for studying the kinetics of electrode reactions in molten salts. The a.c. impedance method involves the measurement of the impedance of the electrode to an alternating current of small amplitude. The relaxation methods involve the displacement of the electrode from its equilibrium potential by perturbation of one of the variables controlling equilibrium. At present, only a small amount of data is available on kinetics of electrode reactions in molten salts; no such data are

available in molten fluorides. Two reviews have been published on electrode processes in molten salts.[22,23] Since the nickel(II)/nickel couple is of importance in this work, previous studies of the kinetics of the reaction Ni(II) + 2e = Ni in molten salts will be discussed.

The charge transfer reaction of the nickel(II)/nickel couple has been studied in molten salts by three groups. Randles and White[24] studied the reaction Ni(II) + 2e + Hg = Ni(Hg) in a nitrate melt at 140° by the a.c. impedance method. The rate constant was reported to be 4.2×10^{-3} cm/sec for an amalgam electrode and 6.2×10^{-3} cm/sec for a pure mercury electrode. The transfer coefficient was found to be 0.41. The addition of water to the melt caused a slight decrease in rate constant while the addition of chloride ions caused a slight increase in rate constant. Addition of bromide ions caused a large increase in rate constant.

Laitinen, Tischer and Roe[25] have measured the charge transfer rate constant for the nickel(II)/nickel couple in a molten KCl-LiCl eutectic at 450° by the double pulse galvanostatic method. Values given for the rate constant and transfer coefficient were 0.1 cm/sec and 0.25, respectively.

Delimarskii, Shapoval and Gorodyskii[26] have reported a series of exchange current measurements on the nickel(II)/nickel couple obtained by the a.c. impedance method. These values yield a rate constant of 1.8×10^{-3} cm/sec and a transfer coefficient of 0.5 for the nickel(II)/nickel couple in NaCl-KCl at 710°.

B. REVIEW OF BASIC PRINCIPLES

1. Electrode Potentials

The equilibrium potential for a reversible redox couple, Ox/Red, is given by the Nernst equation:

$$E_{eq} = E^\circ + \frac{RT}{nF} \ln {}^{a}O/a_R \qquad (1)$$

where

E° = standard potential of the electrode couple, volts

R = universal gas constant (8.315 joules mole^{-1} degree^{-1})

F = faraday (96,487 coulombs)

T = absolute temperature

n = number of electrons involved in the electrode reaction

a_O = activity of the oxidized form

a_R = activity of the reduced form

If the reduced form, Red, is the metallic state, the equilibrium potential for a metal ion/metal electrode is given by the expression:

$$E_{eq} = E^\circ + \frac{RT}{nF} \ln a_{M^{+n}} \qquad (2)$$

In dilute solutions a standard state is generally chosen such that the activity coefficient of the solute approaches unity as the solution approaches infinite dilution; therefore, the activity of the metal ion can be closely approximated by the concentration of the metal ion, $[M^{+n}]$. Equation (2) can then be expressed as

$$E_{eq} = E^\circ + \frac{RT}{nF} \ln [M^{+n}] \qquad (2a)$$

Three concentration scales, molarity (M), molality (m) and mole fraction (X), are widely employed for expressing concentrations in molten salt solutions. Assuming that the number of moles of solute is negligible compared to the number of moles of solvent and that the density of the solution is approximately equal to that of the solvent, the three concentration expressions are given by

$$X = \frac{W_A \, (\overline{GFW})_B}{W_B \, (GFW)_A} \tag{3}$$

$$M = \frac{W_A \, \rho}{W_B \, (GFW)_A} \, 10^3 \tag{4}$$

$$m = \frac{W_A}{W_B \, (GFW)_A} \, 10^3 \tag{5}$$

where

W_A = weight of solute, g

W_B = weight of solvent, g

$(GFW)_A$ = gram formula weight of solute, g/mole

$(\overline{GFW})_B$ = average gram formula weight of solvent, g/mole

ρ = density of solvent, g/ml

From equations (3), (4) and (5), molarity and molality can be expressed in terms of the mole fraction:

$$M = \frac{X\rho}{(\overline{GFW})_B} \, 10^3 \tag{6}$$

$$m = \frac{X}{(\overline{GFW})_B} \, 10^3 \tag{7}$$

At 500° the density of the $LiF-BeF_2-ZrF_4$ (65.6-29.4-5.0 mole per cent) melt is 2.44 g/ml;[27] the average gram formula weight is 39.2 g/mole. Thus, for this melt

$$M = 62.2X$$

$$m = 25.5X$$

At 500° the density of the LiF-NaF-KF (46.5-11.5-42.0 mole per cent) melt is 2.17 g/ml;[28] the average gram formula weight is 41.3 g/mole. Thus, for this melt

$$M = 52.6X$$

$$m = 24.2X$$

For the metal ion/metal couple, the relationships between the standard electrode potentials for the standard states of the different concentration scales, hypothetical unit mole fraction, unit molar and unit molal solutions, are[29]

$$E^\circ_M = E^\circ_X + \frac{RT}{nF} \ln {}^{X}/_{M} \tag{8}$$

$$E^\circ_m = E^\circ_X + \frac{RT}{nF} \ln {}^{X}/_{m} \tag{9}$$

Substitution of equations (6) and (7) into the above expressions gives

$$E^\circ_M = E^\circ_X - \frac{RT}{nF} \ln \frac{\rho\ 10^3}{(\overline{GFW})_B} \tag{8a}$$

$$E^\circ_m = E^\circ_X - \frac{RT}{nF} \ln \frac{10^3}{(\overline{GFW})_B} \tag{9a}$$

For the case Ox + ne = Red, where both Ox and Red forms are soluble species, the standard electrode potential is the same on any concentration scale since the standard state for both species is the same.

For two metal ion/metal couples with ions N^{+z} and L^{+y}, respectively, the relationship for converting the relative standard electrode potentials from the mole fraction concentration scale to the molarity scale is given by

$$E^{\circ}_{M}(N) - E^{\circ}_{M}(L) = E^{\circ}_{X}(N) - E^{\circ}_{X}(L) + \left(\frac{1}{y} - \frac{1}{z}\right) \frac{RT}{F} \ln \frac{\rho\, 10^{3}}{(\overline{GFW})_{B}} \qquad (10)$$

A similar relationship is readily derived from equation (9a) for converting the relative standard electrode potentials from the mole fraction to the molality concentration scale.

2. The Voltage-Step Method

The voltage-step method, a relaxation method for the study of fast electrode reactions, was developed by Vielstich and Delahay[30] as an instrumental simplification of the potential-step method of Gerischer and Vielstich.[31] In this method, a small voltage step is applied rapidly to a cell consisting of a microelectrode at its equilibrium potential and a large non-polarizable counter electrode. The resulting current is measured as a function of time. Linear diffusion is assumed to be the sole mode of mass transport. The overpotential η (the difference between the actual potential and equilibrium potential) applied to the microelectrode varies with current and is given by[30]

$$\eta = V + iR_{t} \qquad (11)$$

where

V = applied voltage step, volts

i = current, amperes (current is positive when V is cathodic or negative)

R_t = total circuit resistance, ohms

η = overpotential, volts

The kinetic parameters of the electrode reaction at the microelectrode are determined from the current-time curves that are recorded on an oscilloscope. If the overpotential is much smaller than $\frac{RT}{\alpha nF}$ (α is the transfer coefficient), the current-time relationship at sufficiently short times can be approximated by[23]

$$i = \frac{-i_o AV}{i_o AR_t + RT/nF}\left(1 - \frac{2\lambda}{\pi^{1/2}} t^{1/2}\right) \qquad (12)$$

i_o = exchange current density, amperes/cm^2

λ = a time-independent parameter that involves the quantities in equation (12) as well as the concentrations and diffusion coefficients of the electroactive species

t = time elapsed after the application of the voltage step, sec

A = area of the microelectrode, cm^2

This relationship, which indicates that current is a linear function of $t^{1/2}$, holds for relatively short time intervals after the initiation of electrolysis and is gradually superseded by a relationship involving $t^{-1/2}$ which holds for pure diffusion control. Equation (12) applies only to a simple one-step electrode process and neglects the charging of the double layer. Charging of the double layer is usually accomplished quickly, especially in molten salts where the cell resistances are low, and, therefore, the charging current quickly becomes negligible in comparison to the faradaic current. The charging current i_{ch} is given by

the expression for the charging of a capacitor:[25]

$$i_{ch} = \frac{V}{R_t} \exp\left(\frac{-t}{R_t C_{dl}}\right) \tag{13}$$

where C_{dl} is the double layer capacitance in farads.

Figure 1 shows a representative current-time curve obtained by the voltage-step method. To determine the exchange current density i_o, the linear portion of the plot of current versus the square root of time, Figure 2 is extrapolated to zero time where $i_{t=o}$ is given by

$$i_{t=o} \frac{-i_o AV}{i_o AR_t + RT/nF} \tag{14}$$

The exchange current density i_o is readily calculated from equation (14).

The use of an effective zero time, t_{eff}, has been suggested by Laitinen, Tischer and Roe.[25] Since initially the faradaic current is zero (the double layer is being charged) and then rises to a maximum before it decays linearly with the square root of time, equation (12) is not valid to zero time. An empirical approximation of t_{eff} is made by placing a vertical line on the current-time curve, Figure 1, such that the area A enclosed to the left of the vertical line by the faradaic current line is equal to the area B enclosed to the right of the vertical line by the faradaic current line and the extrapolated current line transposed from Figure 2.

Oldham and Osteryoung,[32] have made an analysis of the voltage-step method and showed that a plot of current versus the square root of time is linear to within 10 per cent only over the region where

$$i \geq 0.7\, i_{t=o}$$

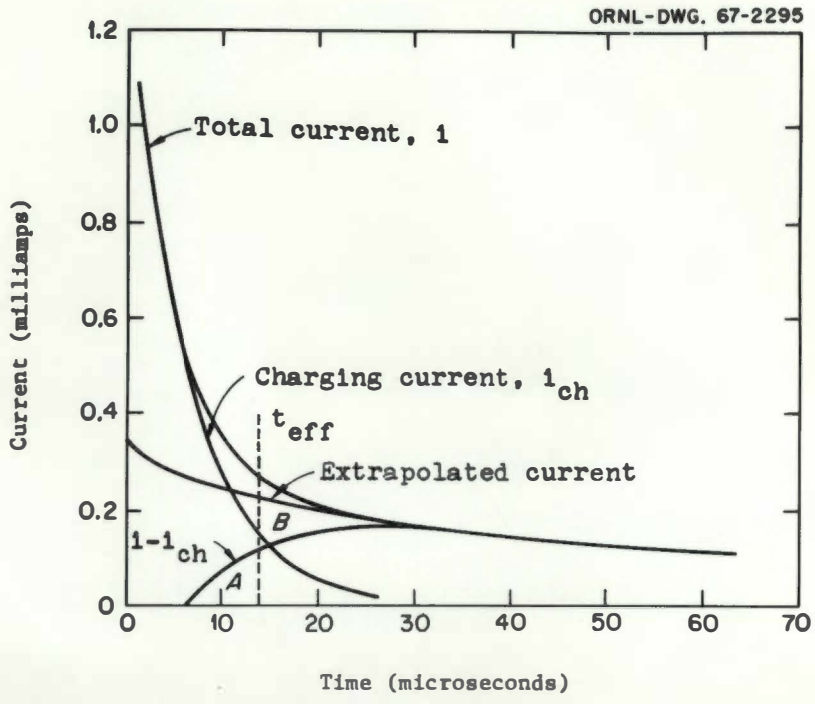

Figure 1. Current-time curves obtained by the voltage-step method.

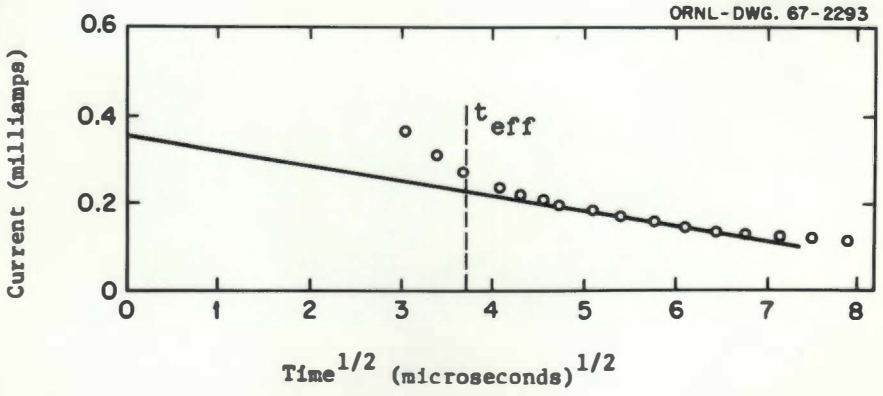

Figure 2. Plot of faradaic current versus the square root of time.

or, when the current is extrapolated to t_{eff}, only where

$$i \geq 0.7\, i_{t_{eff}}$$

The exchange current density i_o is related to the concentration of the oxidized species C_0 for a metal ion/metal couple by the expression:[23]

$$i_o = nFk^o\, C_0^{1-\alpha} \qquad (15)$$

where

C_0 = concentration of the oxidized species in the bulk of the solution, moles/cm^3

k^o = heterogeneous charge transfer rate constant at the standard potential of the electrode couple Ox/Red, cm/sec

The transfer coefficient is determined from the slope of a plot of log i_o versus log C_0. The rate constant k^o may then be calculated from equation (15).

3. Linear Sweep Voltammetry

In linear sweep voltammetry, the potential of the working electrode is varied linearly with time relative to the potential of the reference electrode. The resulting current, flowing between the working electrode and the counter electrode, is measured as a function of potential. For the reversible electrode reaction

$$Ox + ne = Red$$

where only the Ox form is present initially, both species are soluble, and mass transfer takes place by semi-infinite linear diffusion, a representative current-potential curve is shown in Figure 3. The peak current i_p is given by the relationship:[33]

$$i_p = 0.452 \frac{n^{3/2} F^{3/2}}{R^{1/2} T^{1/2}} A D^{1/2} C v^{1/2} \qquad (16)$$

where

D = diffusion coefficient of the reactant, cm^2/sec

C = bulk concentration of the reactant, $moles/cm^3$

v = rate of potential scan, volts/sec

The voltammetric equivalent of the standard electrode potential, the polarographic half-wave potential $E_{1/2}$, is the potential at which the concentrations of reactant and product are equal at the electrode surface. $E_{1/2}$ corresponds to a potential on the voltammogram at which the current is equal to 85 per cent of i_p (assuming only one species of the redox couple is present initially).[34]

C. PROPOSED RESEARCH

This dissertation deals primarily with the measurement of electrode potentials in molten fluorides. Such measurements require a practical reference electrode. The reference electrode chosen for this investigation consists of the nickel(II)/nickel couple in a fluoride melt, contained in a boron nitride compartment.

The specific purposes of this dissertation are to

(a) demonstrate the utility of the above reference electrode in molten fluorides

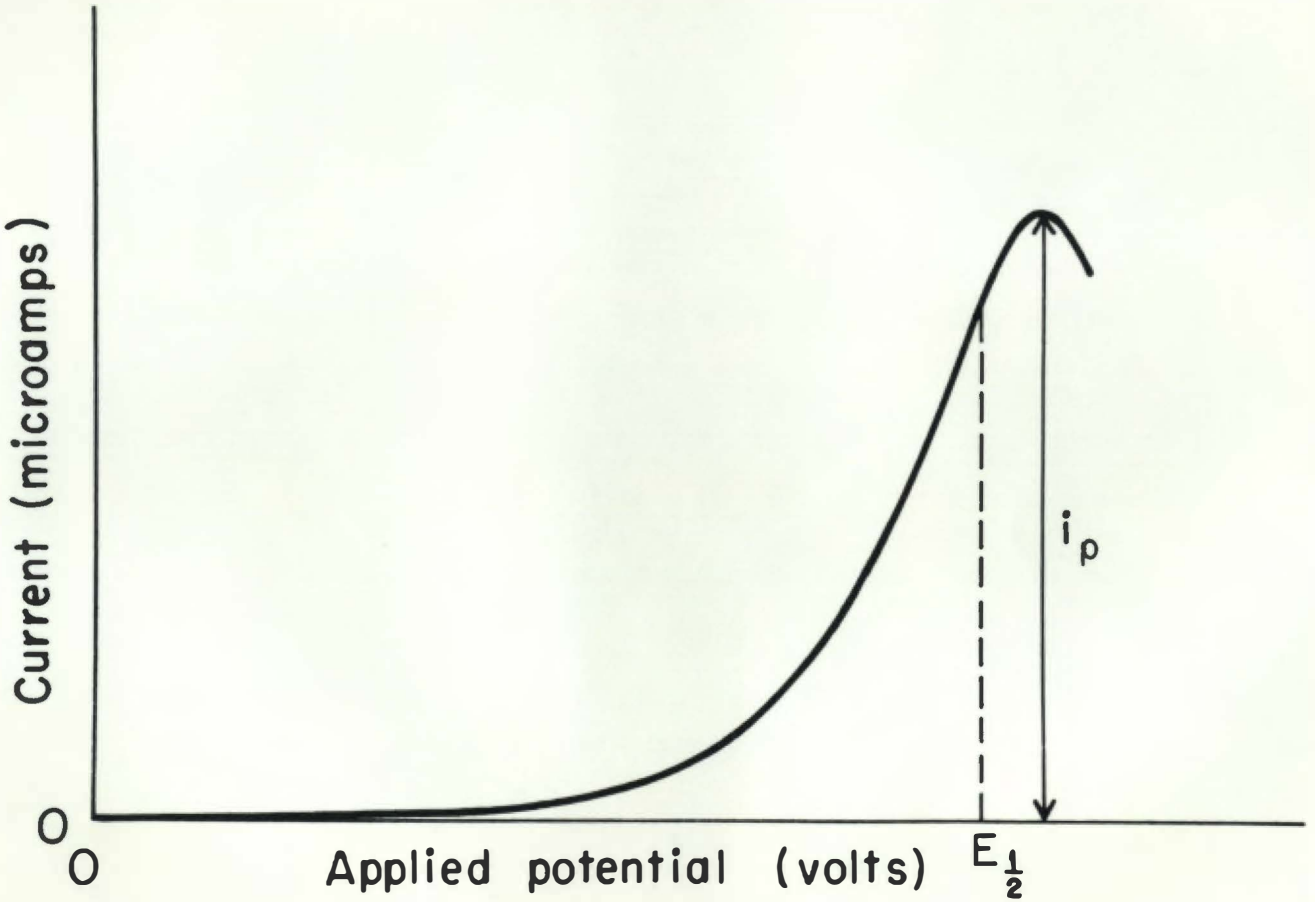

Figure 3. A typical voltammogram.

(b) obtain a measure of the reversibility of the reference electrode couple, nickel(II)/nickel

(c) determine the electrode potentials of several redox couples in molten fluorides by emf measurements.

CHAPTER II

EXPERIMENTAL

A. MATERIALS

Two fluoride salt mixtures were used as solvents in this investigation:

(1) lithium fluoride-sodium fluoride-potassium fluoride (46.5-11.5-42.0 mole per cent, liquidus temperature 454°)[28]

(2) lithium fluoride-beryllium fluoride-zirconium fluoride (65.6-29.4-5.0 mole per cent, liquidus temperature 434°)[27].

These two salt mixtures and the following anhydrous fluoride salts were obtained from the Reactor Chemistry Division of the Oak Ridge National Laboratory:[35] nickel(II) fluoride, iron(II) fluoride, iron(III) fluoride, chromium(II) fluoride, chromium(III) fluoride and lithium fluoride-uranium(IV) fluoride (73-27 mole per cent). None of these solute salts received any further treatment; however, all were stored in an inert atmosphere until their use.

Boron nitride used in the construction of the reference electrodes was grade A or HP (Carborundum Co.). Machining of this material was performed in an open atmosphere with regular metal cutting tools. The boron nitride was kept in a desiccator containing anhydrous calcium chloride, except for the time required for machining.

B. APPARATUS

1. Drybox-Furnace System

A drybox-furnace combination, which provided an inert atmosphere while allowing some freedom in the manipulation of electrodes and the addition of reagents to the melt, was used in this investigation. A photograph of this system is shown in Figure 4. A pot type furnace, approximately five kilowatts heating capacity, was attached to the bottom of the drybox. The bottom of the drybox was covered with water cooled coils, and the coils were covered with a raised floor. A moisture content of 10-20 parts per million (measured with a moisture monitor, Beckman Hygromite Model-97) could be achieved in this system with the continuous circulation of the helium cover gas through a moisture trap (3 in. diameter, 10 in. high) containing 13X Molecular Sieve.

Molten salt was contained in a graphite cup (usually 3.5 in. inner diameter, 5 in. high) held in a one liter borosilicate beaker in order to insulate it from the furnace. Temperature was measured by a platinum/platinum-rhodium (10 per cent) thermocouple immersed in the melt. An on-off type temperature controller maintained the temperature to ±2°.

2. Equipment for Emf Measurements

All emf measurements were made with a Moseley Autograph X-Y recorder Model 2D-2A (input impedance one megohm). In most cases, measurements were made directly with the X-Y recorder; however, in some cases, in order to expand the recorder scales, the emf was first amplified using a Keithley 600A electrometer.

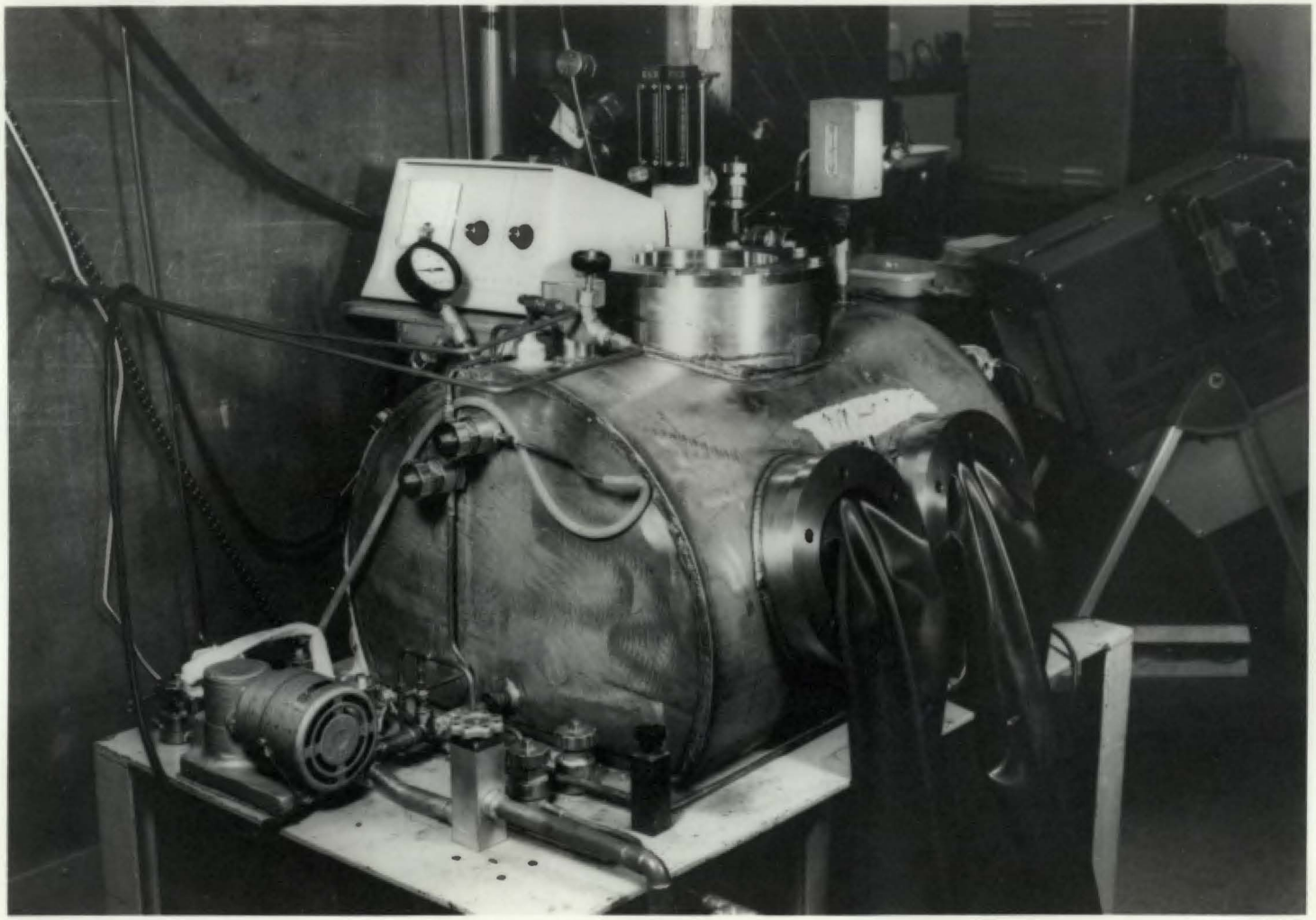

Figure 4. Photograph of the drybox-furnace system.

High purity nickel and iron wires, coiled several times on the end to give a large surface area, were employed as indicator electrodes for the nickel(II)/nickel couple and the iron(II)/iron couple, respectively. The beryllium, zirconium and chromium indicator electrodes were constructed by attaching a threaded 1 to 1.5 in. long piece of the desired metal to a long, 1/8 in. diameter nickel rod. An inert platinum electrode consisted of a 2 in. long, 0.04 in. diameter platinum wire attached by means of a weld to a 1/8 in. diameter nickel rod. The beryllium and zirconium electrodes were cleaned with emory paper and rinsed in acetone. The other electrodes were merely rinsed in acetone and distilled water and dried.

The reference electrode design used in this study is shown in Figure 5. It consisted of the nickel(II)/nickel couple in the fluoride solvent contained in a boron nitride compartment. The compartment, which was 0.5 in. outer diameter and about 3 in. high, had a wall thickness of 1/32 in. in the lower portion and 3/32 in. in the upper portion. A threaded cap of boron nitride pinned to the nickel rod held the nickel rod in place.

3. Equipment for Kinetic Measurements

The microelectrode used in the kinetic measurements was a high purity 0.005 in. diameter nickel wire immersed in the melt to give an area of $\sim$0.01 to 0.02 cm^2. A 0.032 in. diameter nickel wire, coiled several times on the end, was used as the counter electrode.

Figure 6 shows the diagram of the voltage-step circuit used. This circuit was essentially that employed by Laitinen, Tischer and Roe.[25] The desired voltage step was obtained from a voltage divider

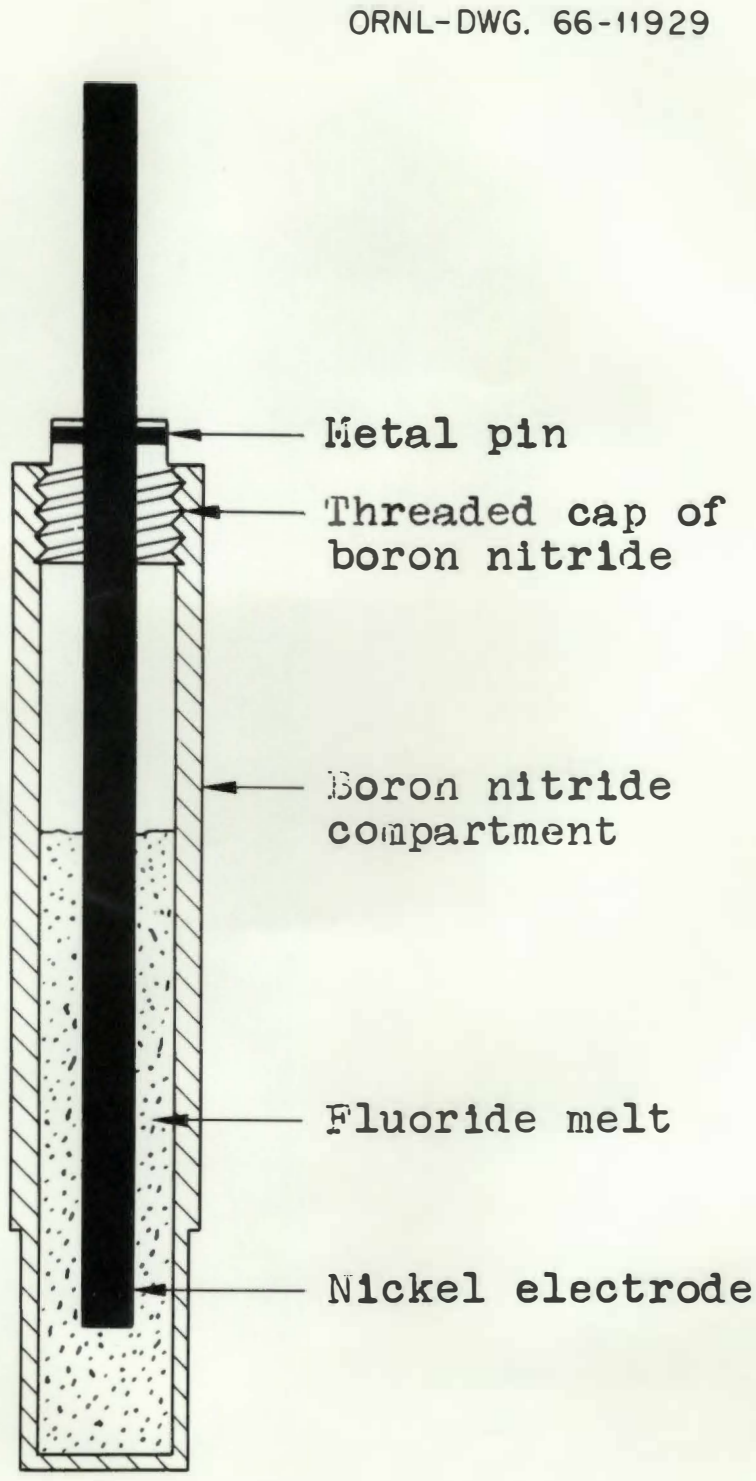

Figure 5. Nickel(II)/nickel electrode in a boron nitride compartment.

ORNL-DWG. 69-284

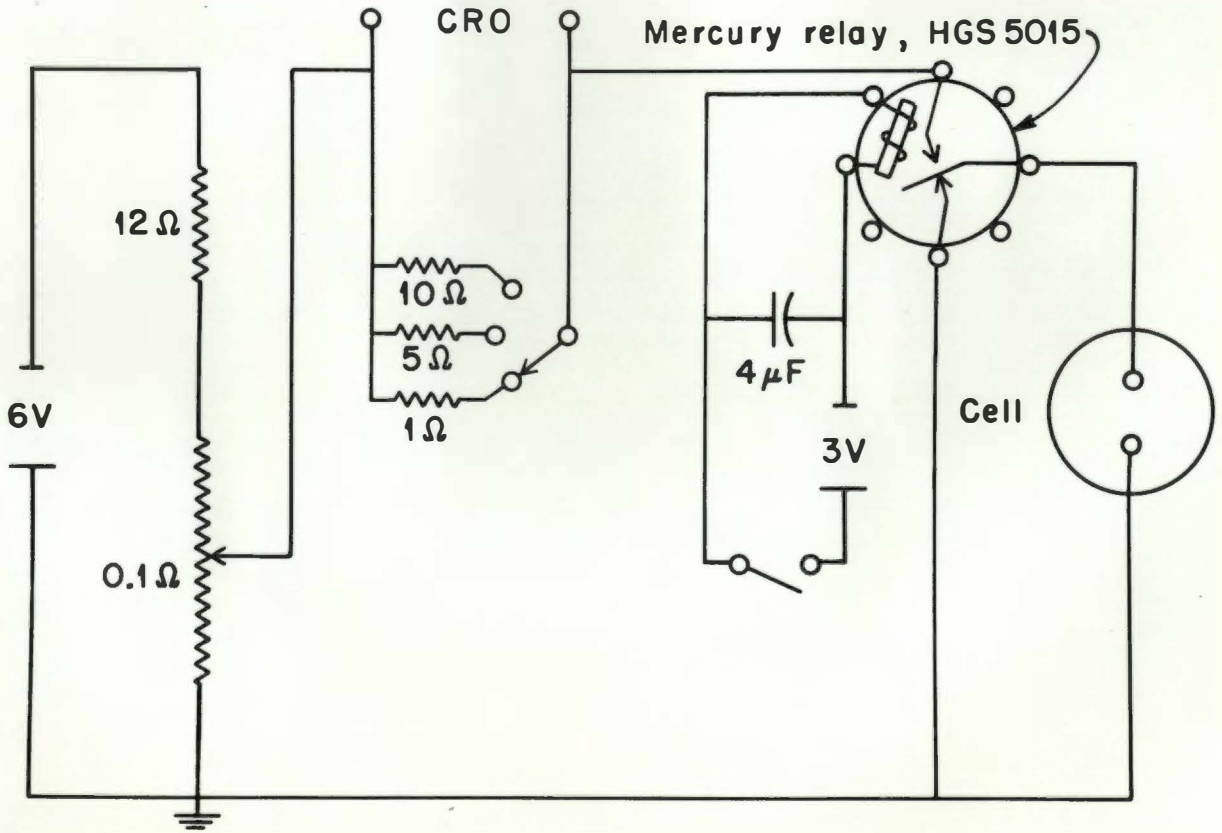

Figure 6. Schematic diagram of the voltage-step circuit.

across a 6 volt storage battery. The cell was initially short circuited; the voltage step was then applied to the cell by switching the mercury relay, a break-before-make type HGS 5015. The resulting current was measured as a voltage drop across a precision resistor. The voltage drop across the resistor was fed into a Tektronix 1A7 plug-in, high gain differential amplifier with a 500 kHz band pass; the voltage-time curves were recorded on a Tektronix 549 storage oscilloscope and photographed with a Tektronix C-12 oscilloscope camera on Polaroid type 42 (ASA 200 speed) film.

4. Equipment for Voltammetric Measurements

A controlled-potential voltammeter equipped with a differentiating circuit[36] was employed for all voltammetric measurements. Current-potential curves were recorded on a Moseley Autograph X-Y recorder Model 2D-2A. Platinum wire (0.02 in. diameter), nickel wire (0.032 in. diameter) and pyrolytic graphite (0.10 cm diameter) working electrodes were used with electrode areas of approximately 0.05 cm^2. The metal wire electrodes were polished with 3/0 emory paper before use. A 0.25 in. diameter graphite rod was employed as a counter electrode; generally, a nickel(II)/nickel reference electrode contained in a boron nitride compartment was used.

C. PROCEDURE

1. Emf Measurements

The graphite cup, borosilicate beaker and boron nitride sheath were heated to 500° under vacuum, overnight in the drybox-furnace

system. After the above pretreatment, the boron nitride compartment was filled with the solvent salt containing a small amount of nickel(II) fluoride, and approximately 300 grams of the solvent salt were placed in the graphite cup. The cell was again heated to 500° under vacuum, and the reference electrode immersed in the melt. After the resistance of the boron nitride decreased to less than 10,000 ohms, the stability of the reference electrode was established over a 24 to 48 hour period before measurements were made with it. The cell assembly employed for emf measurements is shown in Figure 7, in this case for a nickel(II)/nickel concentration cell.

Voltammetric current-potential curves were recorded in each melt and used to identify impurities and approximate their concentrations. Removal of the common ion impurities, nickel(II), iron(II) and chromium(II), in the LiF-BeF_2-ZrF_4 melt was accomplished by reduction with zirconium metal immersed in the melt. In the LiF-NaF-KF melt, removal of these impurities was accomplished by controlled potential pre-electrolysis employing either a 0.25 in. diameter graphite rod or a platinum gauze as the cathode.

In most cases, emf measurements were made as a function of concentration; the concentration of the solute species was varied by addition of the anhydrous solute salt. It was established from stability of emf measurements and from variations in i_p on voltammograms that homogeneity of solutions was attained by waiting about one hour between additions and measurements; the melt was stirred periodically (either manually or mechanically) during that time. Emf measurements were

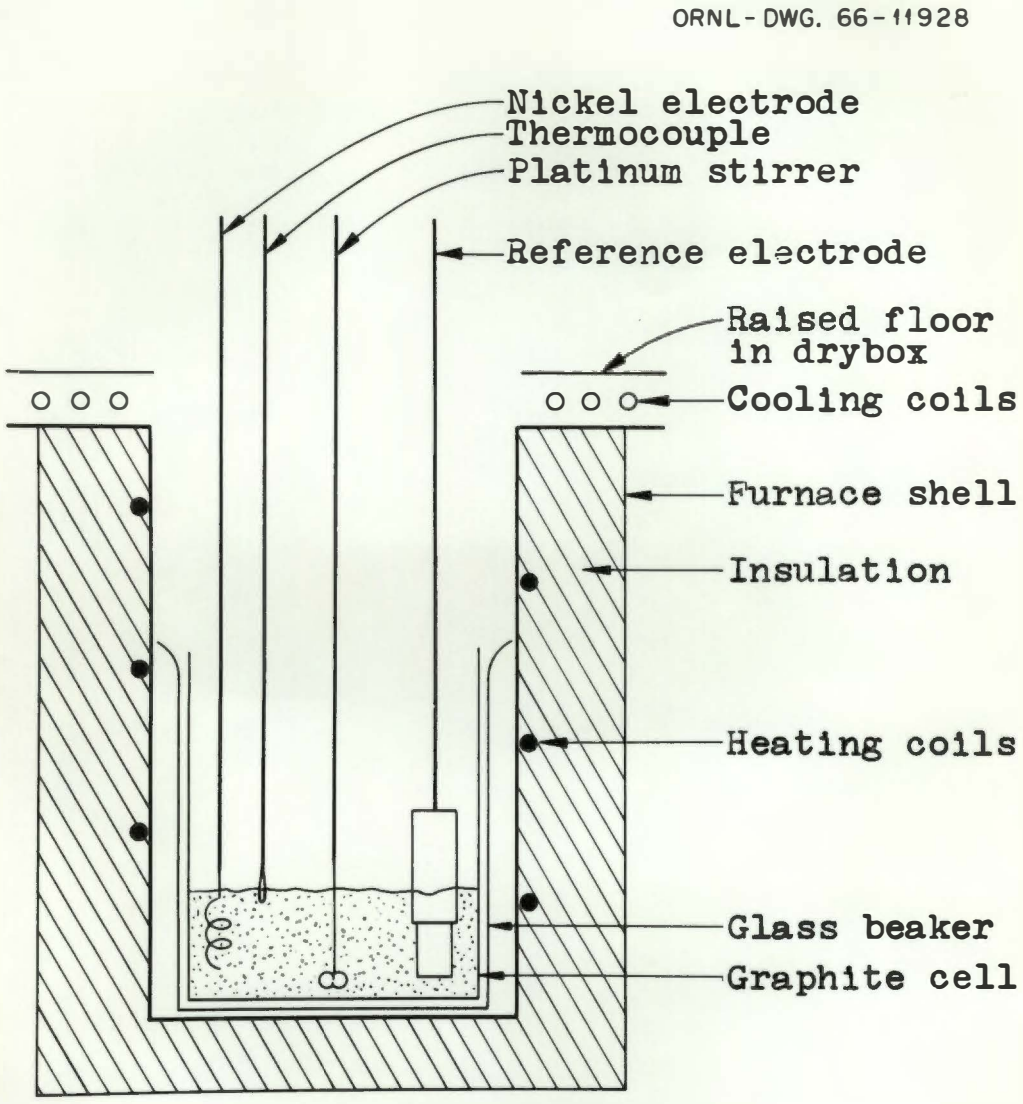

Figure 7. Cell assembly for emf measurements.

recorded over a 15 to 30 minute period to insure the stability of the values. The uranium(III) concentration was varied by the controlled reduction of uranium(IV) with a zirconium rod immersed in the melt.

Solute concentration was determined in most cases either by spectrophotometric analysis of a sample taken at the time of the corresponding emf measurement (all analyses were performed by the General Analyses Laboratory, Analytical Chemistry Division, the Oak Ridge National Laboratory) or from a voltammetric current-potential curve recorded at the time of the corresponding emf measurement. The uranium(III) and uranium(IV) concentrations were determined from spectrophotometric analysis of molten salt samples taken in graphite windowless cells.[37] These measurements were made by Dr. J. P. Young of the Analytical Chemistry Division of the Oak Ridge National Laboratory. Each sample was allowed to solidify and transferred to a heated spectrophotometric facility. The complete operation was performed without exposing the sample to the atmosphere.

2. Voltage-Step Measurements

The performance of the voltage-step circuit was verified on a "dummy" cell, a 0.47 μF capacitor (20 per cent tolerance) in series with a 5 ohm precision resistor. The experimentally determined value of the resistor was 5.1 ohms (including the circuit resistance), and the experimentally determined value of the capacitor was 0.45 μF. Pretreatment of the molten salt was the same as that employed in emf measurements. The distance between the microelectrode and the counter electrode was less than 1 cm in all experiments.

The total resistance of the circuit and the electrode double layer capacitance were determined by means of equation (13), page 16 from a current-time curves obtained in a blank solution. Current-time curves were obtained as a function of the nickel(II) concentration by making additions of anhydrous nickel(II) fluoride; concentrations were determined spectrophotometrically on samples taken after recording each current-time curve.

Measurements were generally made across a 1 ohm precision resistor and recorded on the oscilloscope using the sensitivity of 0.2 mV/cm and at a sweep rate of 10 μsec/cm. The current-time curves were photographed, enlarged approximately 2.5 times and traced onto graph paper for the determination of exchange current densities.

CHAPTER III

RESULTS AND DISCUSSION

A. EMF MEASUREMENTS ON THE NICKEL(II)/NICKEL COUPLE

1. Considerations for a Reference Electrode

The nickel(II)/nickel couple was chosen as the electrode couple for a reference electrode for several reasons. Nickel exhibits only one stable oxidation state in fluoride solutions, nickel(II). The nickel(II)/nickel couple is rather noble, and its potential is approximately in the middle of the potential range in alkali metal fluorides (column VI of Table I, page 6). In addition, this couple has been employed previously by other investigators as a reference electrode in fluoride solvents.[15,16]

A boron nitride compartment was chosen to isolate the nickel(II)/nickel reference couple from the bulk of the melt. Although boron nitride has a resistivity of about 2.3×10^{10} ohm-cm at 500°,[38] its electrical conductivity increases as it becomes impregnated with the molten fluoride salt. Therefore, this arrangement should provide ionic contact between the reference couple and the bulk of the melt while limiting diffusion between the half-cells.

2. Nernstian Reversibility Measurements

The applicability of the Nernst equation to the nickel(II)/nickel couple was investigated in the two solvent salts using the

following concentration cell:

$$\text{Ni/Ni(II)}\ (a_1 = \text{constant})\ \underset{\text{sheath}}{\overset{\text{boron}}{//\text{nitride}//}}\ \text{Ni(II)}\ (a_2)\text{/Ni}$$

The activity of the nickel(II) in the boron nitride compartment, a_1, was constant. Thus, the emf of the cell is given by the expression:

$$E_{cell} = \frac{RT}{nF} \ln a_2/a_1 + E_j \qquad (17)$$

where E_j is the junction potential across the boron nitride wall separating the two half-cells. Assuming any junction potential at a given temperature and the activity coefficient over the concentration range studied (approximately 10^{-4} to 10^{-3} mole fraction) to be constant, the cell emf is given by the expression:

$$E_{cell} = \frac{RT}{nF} \ln X_2 + \text{constant} \qquad (17a)$$

where X_2 is the mole fraction of nickel(II) in the bulk of the melt.

Plots of E_{cell} versus log X_2 are shown in Figure 8 for measurements made in LiF-NaF-KF (A) and in LiF-BeF_2-ZrF_4 (B). These results are summarized in Table II. The lines drawn through the data points have the theoretical slopes, $\frac{2.3\ RT}{nF}$, of 0.078 (A) and 0.077 (B) as given by the Nernst equation.

3. Performance of the Reference Electrode

The wetting characteristics of the boron nitride compartments in the two solvents were found to be quite different. In LiF-NaF-KF, the boron nitride compartment was penetrated by the melt rather quickly; resistance decreased to less than 1000 ohms in approximately 24 to 48 hours at 500°. In LiF-BeF_2-ZrF_4, usually 10 to 14 days were required for the resistance to decrease to less than 10,000 ohms

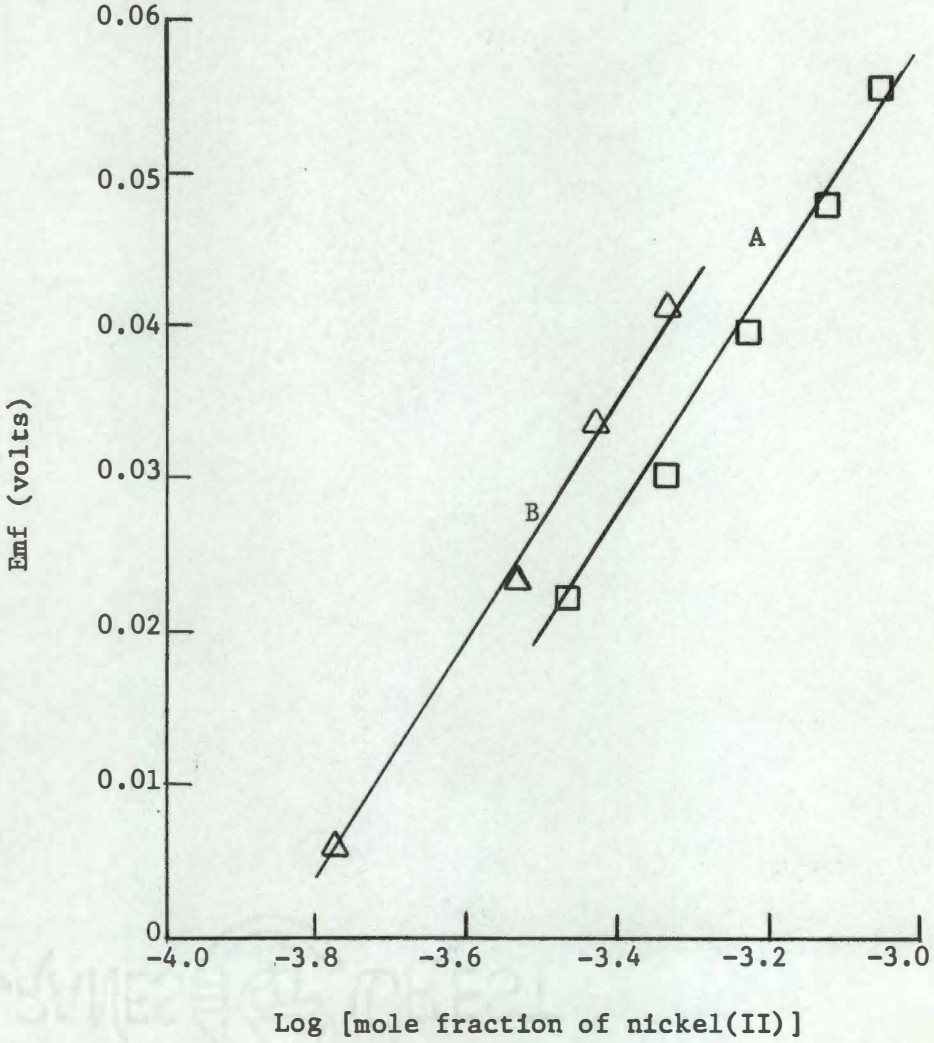

Figure 8. Nernstian plots for the nickel(II)/nickel couple: (A) in LiF-NaF-KF at 517°, (B) in LiF-BeF_2-ZrF_4 at 507°.

TABLE II

SUMMARY OF EMF MEASUREMENTS ON THE NICKEL(II)/NICKEL COUPLE

[Ni(II)], mole fraction	$E_{ref}-E_{Ni(II)/Ni}$, volts
1.67×10^{-4}[a]	-0.0058
2.91×10^{-4}[a]	-0.0232
3.70×10^{-4}[a]	-0.0335
4.59×10^{-4}[a]	-0.0411
3.39×10^{-4}[b]	-0.0223
4.62×10^{-4}[b]	-0.0302
5.83×10^{-4}[b]	-0.0395
7.46×10^{-4}[b]	-0.0479
8.72×10^{-4}[b]	-0.0556

[a] In LiF-NaF-KF at 517°.

[b] In $LiF-BeF_2-ZrF_4$ at 507°.

at 500°. Since boron nitride compartments which were not pretreated to remove adsorbed moisture wet quickly in both solvents, the wetting ability of the two solvents appears to be related to the free oxide content of the melt.

Measurements in $LiF-BeF_2-ZrF_4$ indicated that in some cases a significant junction potential existed across the boron nitride wall and that this potential was temperature dependent. These measurements were made with the same nickel(II) concentration inside the boron nitride compartment and in the bulk of the melt. Under these circumstances, the cell emf as given by equation (17), page 34, is

$$E_{cell} = E_j$$

For a nickel(II) concentration of $\sim 8.9 \times 10^{-5}$ mole fraction, the potential of the reference electrode at 500° was about 25 mV anodic to the nickel(II)/nickel electrode in the bulk of the melt. In another instance, for a nickel(II) concentration of $\sim 8.0 \times 10^{-4}$ mole fraction, the potential of the reference electrode at 500° was about 105 mV cathodic to the nickel(II)/nickel electrode in the bulk of the melt. The junction potential of the latter cell changed from ~ 100 mV to ~ 120 mV on increasing the temperature of the melt from 480° to 550°. From voltammetric measurements of the position of the nickel(II) reduction wave with respect to the reference electrode in boron nitride and another nickel(II)/nickel electrode in the bulk of the melt, it was shown that the variation in the cell emf was caused by the variation in the potential of the reference electrode, in other words, variation of the junction potential. It appears that the variations in junction potential between reference electrodes contained in boron nitride are

due to such factors as atmospheric exposure, machining variations, pretreatment and variations between batches of boron nitride.

In the cell described above (8.0×10^{-4} mole fraction nickel(II) in both half-cells), the cell emf (in this case junction potential) was stable over a two week period at 0.11 ± 0.01 V. The emf's of other concentration cells at constant composition were also observed to be reasonably stable for several days. In $LiF-BeF_2-ZrF_4$ at 492°, the emf was constant to within $\pm$ 6 mV over a twelve day period; in LiF-NaF-KF at 505°, the cell emf was stable to within $\pm$ 3 mV over an eleven day period.

Since emf measurements on a redox couple are usually made over a period of a few days, it appears that a reference electrode isolated in a boron nitride compartment is useful in spite of the inclusion of an unpredictable junction potential. However, in order to relate measured emf's to the common reference point, the standard electrode potential of the nickel(II)/nickel couple (standard state of nickel(II) was taken to be the hypothetical unit mole fraction solution), it was necessary in each experiment to measure the potential of the reference electrode with respect to a nickel(II)/nickel electrode in the bulk of the melt. Many of the salts used in this investigation initially contained a significant concentration of nickel(II), up to a 1×10^{-4} mole fraction. In these cases, it was a simple matter to make an emf measurement between the reference electrode and a nickel(II)/nickel electrode in the bulk of the melt. By means of the Nernst equation, the potential of the reference electrode was related to the standard electrode potential

of the nickel(II)/nickel couple. In other instances, where the nickel(II)/nickel couple was stable in the presence of the other electroactive species, for example iron(II) and zirconium(IV), the potential of the reference electrode was related to the potential of a nickel(II)/nickel electrode after emf measurements had been made between the reference electrode and the other couple. This was done by varying the nickel(II) concentration in the bulk of the melt and measuring the emf between the nickel(II)/nickel electrode and the reference electrode employed in the previous measurements. Again the potential of the reference electrode was related to the standard electrode potential of the nickel(II)/nickel couple by the Nernst equation.

B. KINETIC MEASUREMENTS ON THE NICKEL(II)/NICKEL COUPLE

Since the nickel(II)/nickel couple was employed as the electrode couple in a reference electrode, it was desirable to obtain a quantitative measure of the reversibility of the charge transfer reaction

$$Ni(II) + 2e = Ni$$

The voltage-step method was chosen for this investigation due to the simplicity of the required instrumentation.

1. Measurement of Circuit Resistance and Double Layer Capacitance

The total circuit resistance R_t and the double layer capacitance C_{dl} were determined from current-time curves obtained in a blank

solution. Such current-time curves represent only the charging of the double layer capacitance; the current-time relationship is given by equation (13), page 16. Figure 9 shows two such curves obtained in $LiF-BeF_2-ZrF_4$ at 500° for different voltage steps, (area of nickel wire miroelectrode = 0.022 cm^2). Figure 10 shows the data from Figure 9 plotted as log i versus time. Values of R_t were calculated by extrapolating the lines in Figure 10 to zero time where

$$R_t = \frac{\text{Voltage step}}{i_{t=0}}$$

Both lines yield a value of 7.34 ohms for R_t. This value included a 5.00 ohm measuring resistor in the circuit; therefore, neglecting other circuit resistance, the cell resistance was 2.34 ohms.

The double layer capacitance was calculated from the slope of the lines in Figure 10 which is given by

$$\text{Slope} = -1/R_t C_{dl}$$

C_{dl} was found to be 33.7 $\mu F/cm^2$. In preliminary experiments, the nickel microelectrode consisted of a nickel wire sheathed with boron nitride so that only the end cross section was exposed to the melt. With this type of microelectrode, double layer capacitance was observed to be much greater than without the sheath, $\sim$ 100 to 200 $\mu F/cm^2$. Apparently the presence of the boron nitride sheath enhances adsorption at the electrode surface which increases the value of the double layer capacitance.

ORNL-DWG. 69-682

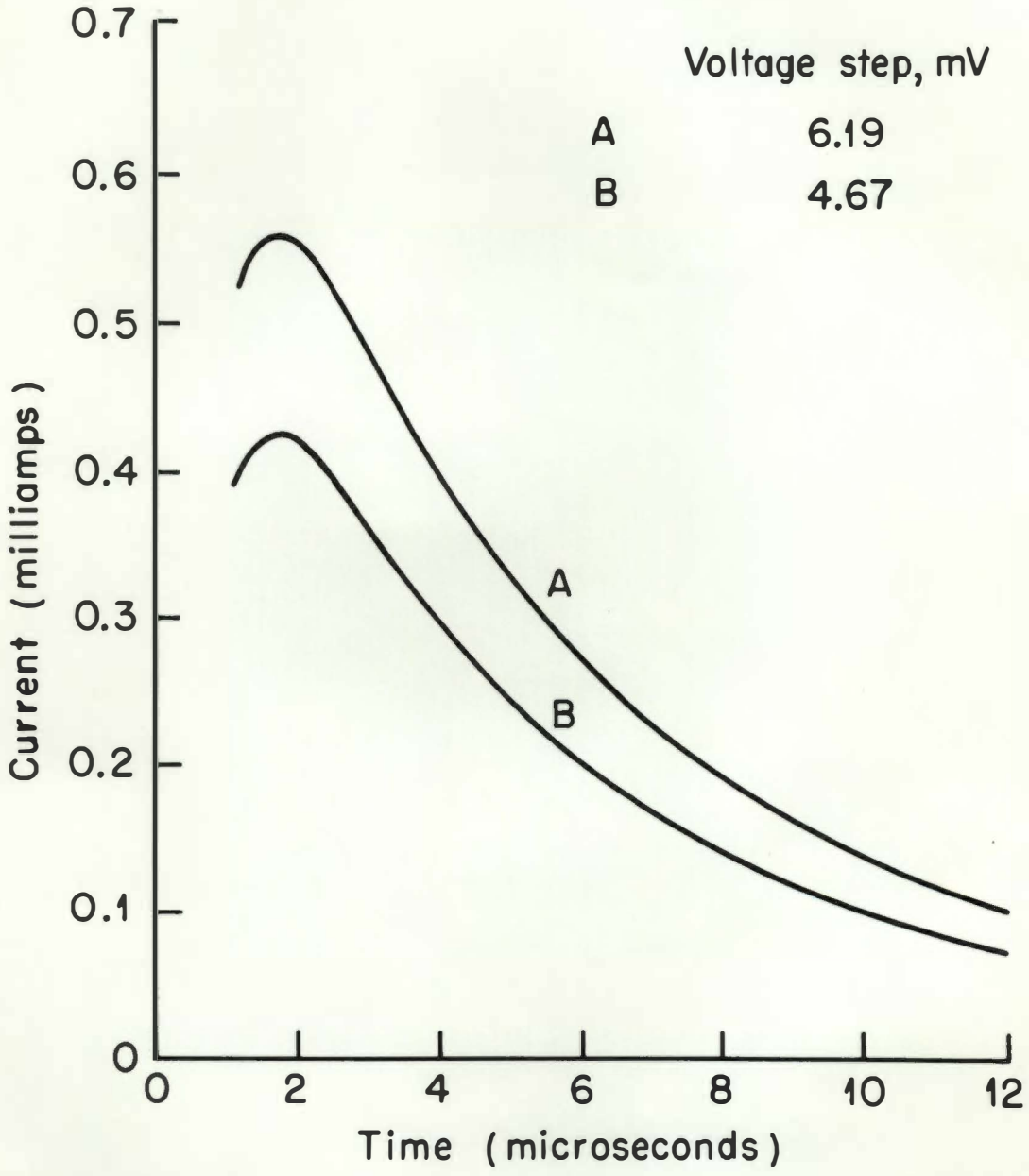

Figure 9. Charging current-time curves obtained by the voltage-step method in $LiF-BeF_2-ZrF_4$ at 500°.

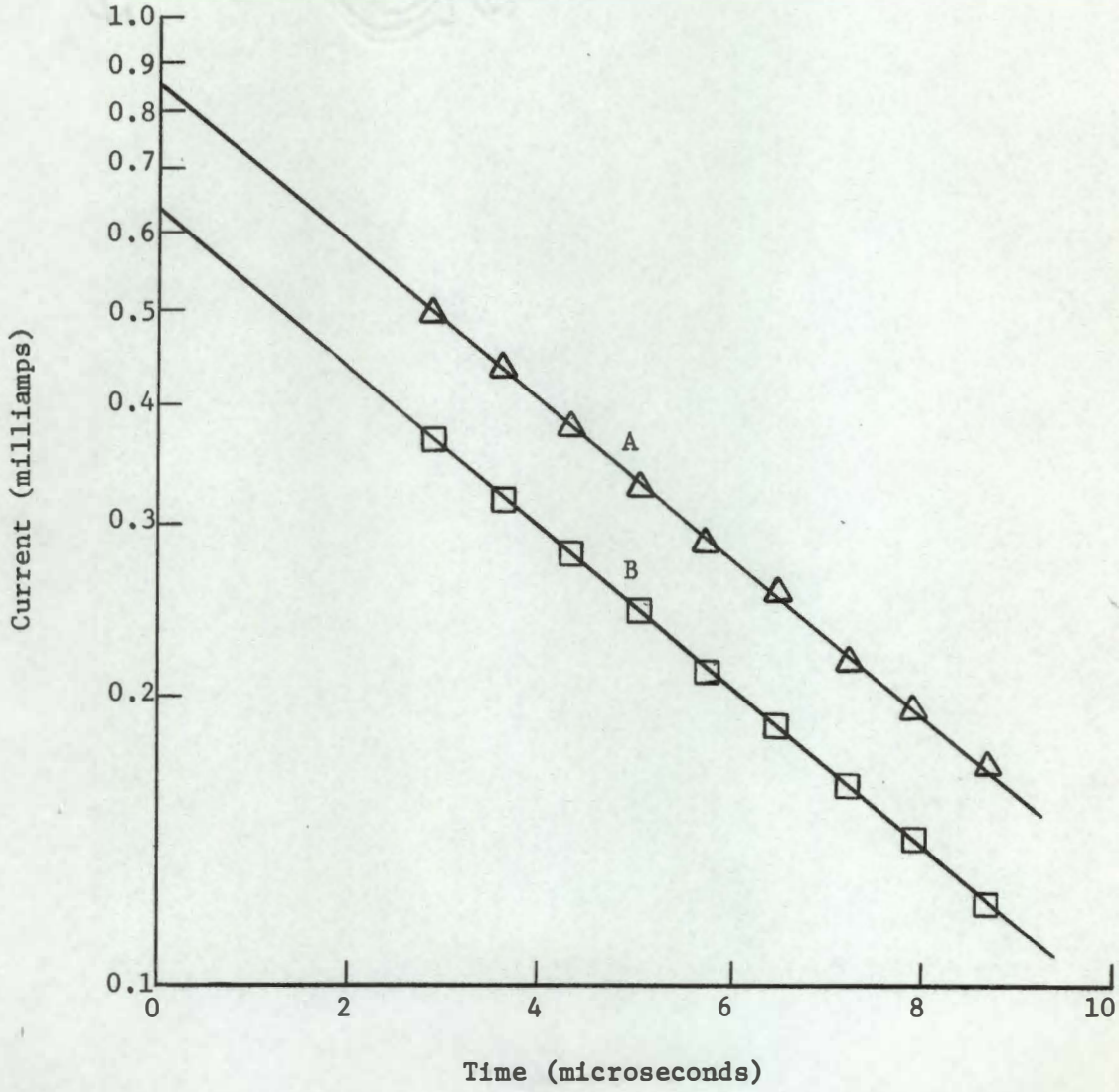

Figure 10. Plot of log [charging current] versus time.

2. Determination of the Kinetic Parameters

Figure 11 shows two of the current-time curves obtained in solutions of nickel(II) in $LiF-BeF_2-ZrF_4$ at 500° (area of nickel wire microelectrode = 0.022 cm^2). A comparison of these current-time curves (R_t = 3.34 ohms including a 1.00 ohm measuring resistor) with the double layer charging curves in Figure 9, page 41, (R_t = 7.34 ohms including a 5.00 ohm measuring resistor) indicates a large increase in current at the short times. This increase in current indicates a significant increase in the apparent double layer capacitance which in turn indicates the adsorption of nickel(II) at the microelectrode. It has been shown that only a small amount of reactant adsorption is required to produce a large increase in double layer capacitance. For example, Timmer, Sluyters-Rehbach and Sluyters[39] have observed a 40 $\mu F/cm^2$ increase in apparent double layer capacitance for the thallium(I)/thallium(mercury) couple under conditions where measurements have shown less than 1 $\mu C/cm^2$ of thallium(I) is adsorbed.[40]

Matsuda and Delahay[41] have considered the problem of reactant adsorption for the potentiostatic method; however, the separation of the adsorption terms was found to be very difficult. Even in the presence of reactant adsorption, an estimate of the charge transfer rate constant by the application of the voltage-step theory for a simple one-step reaction in the absence of reactant adsorption is formally possible.

Figure 12 shows a plot of i versus $t^{1/2}$ for curves A and B from Figure 11. Data points at the longer times, where the effect of the charging current was least, were extrapolated to zero time for the

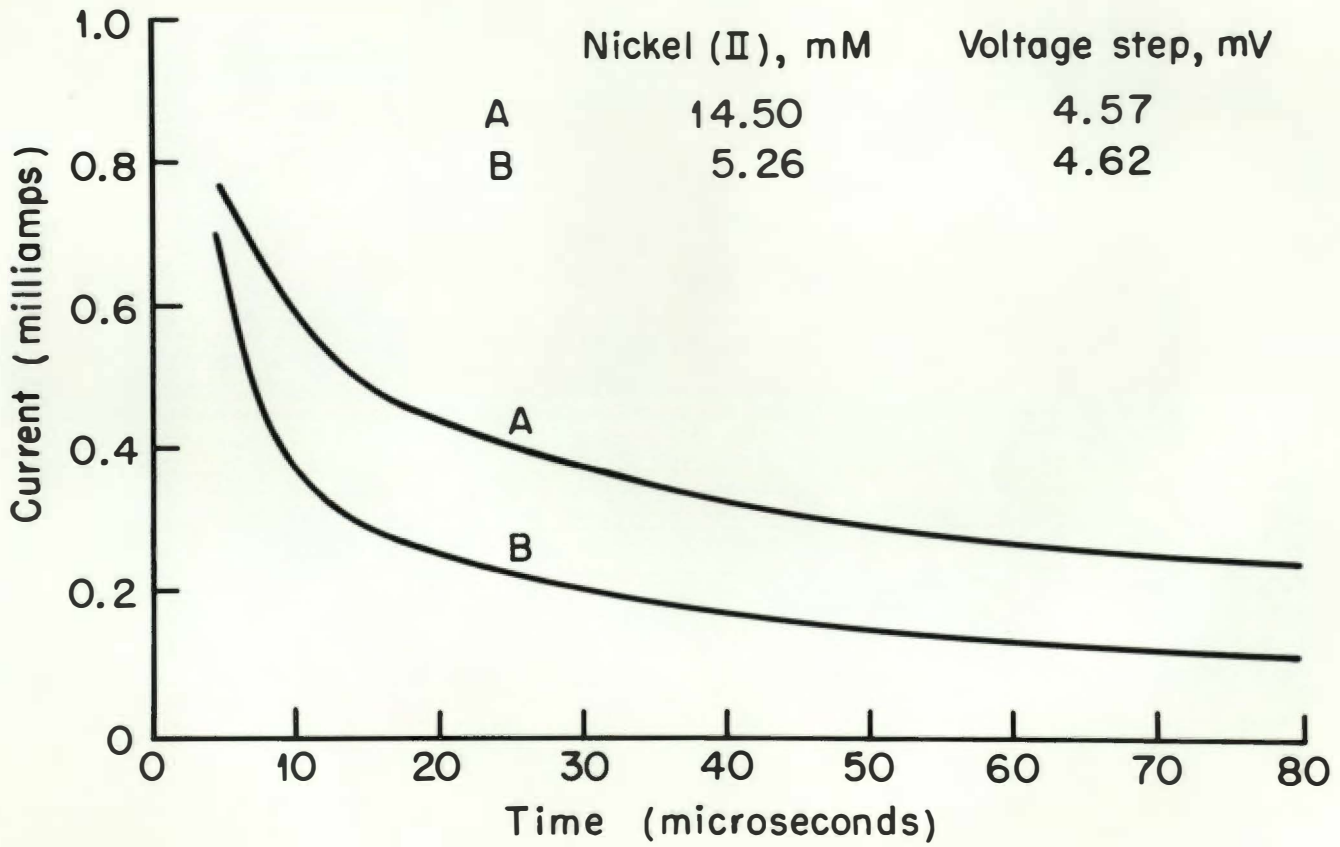

Figure 11. Current-time curves for the reduction of nickel(II) in LiF-BeF_2-ZrF_4 at 500°.

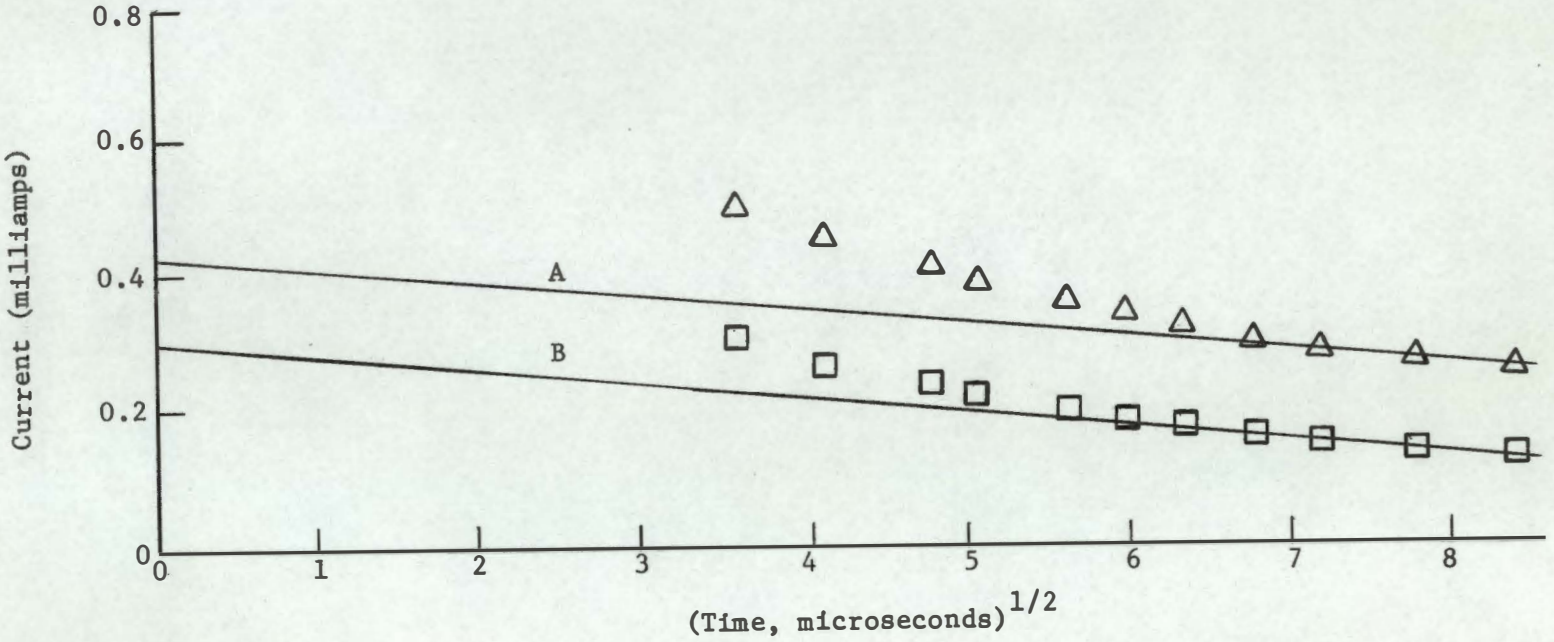

Figure 12. Plot of faradaic current versus the square root of time for the determination of $i_{t=o}$.

evaluation of exchange current densities. The use of the effective zero time suggested by Laitinen, Tischer and Roe[25] could not be applied since the value of the double layer capacitance apparently changed from that determined in the blank solution. Likewise, the considerations of Oldham and Osteryoung[32] were not taken into account due to apparent adsorption of nickel(II).

Figure 13 shows a plot of the log i_o versus the log [nickel(II)]. Exchange current values (see Table III) were determined for the two voltage steps at each concentration of nickel(II). Since the data points did not result in a good straight line, the range of the transfer coefficient α was determined from the slopes of the lines drawn through the extremes of the data points (lines A and B). From equation (15), page 18, the slope of such a line is equal to $1-\alpha$. This produced a range in α of 0.32 to 0.55. The corresponding range in the heterogeneous rate constant k°, calculated from equation (15), was 1.6×10^{-4} to 2.3×10^{-3} cm/sec. Approximately the same range in rate constant was observed in LiF-NaF-KF at 500°.

Although a rate constant in the range determined for the nickel(II)/nickel couple in this study may be considered to correspond to a reversible (or quasi-reversible) process provided the current is small,[33] it is considerably lower than rate constants for metal ion/metal couples in KCl-LiCl at 450°. A rate constant of 0.1 cm/sec was reported in that study for the nickel(II)/nickel couple. However, Randles and White[24] reported a value of 4.2×10^{-3} cm/sec for the nickel(II)/nickel couple in a nitrate melt at 140°, and Delimarskii,

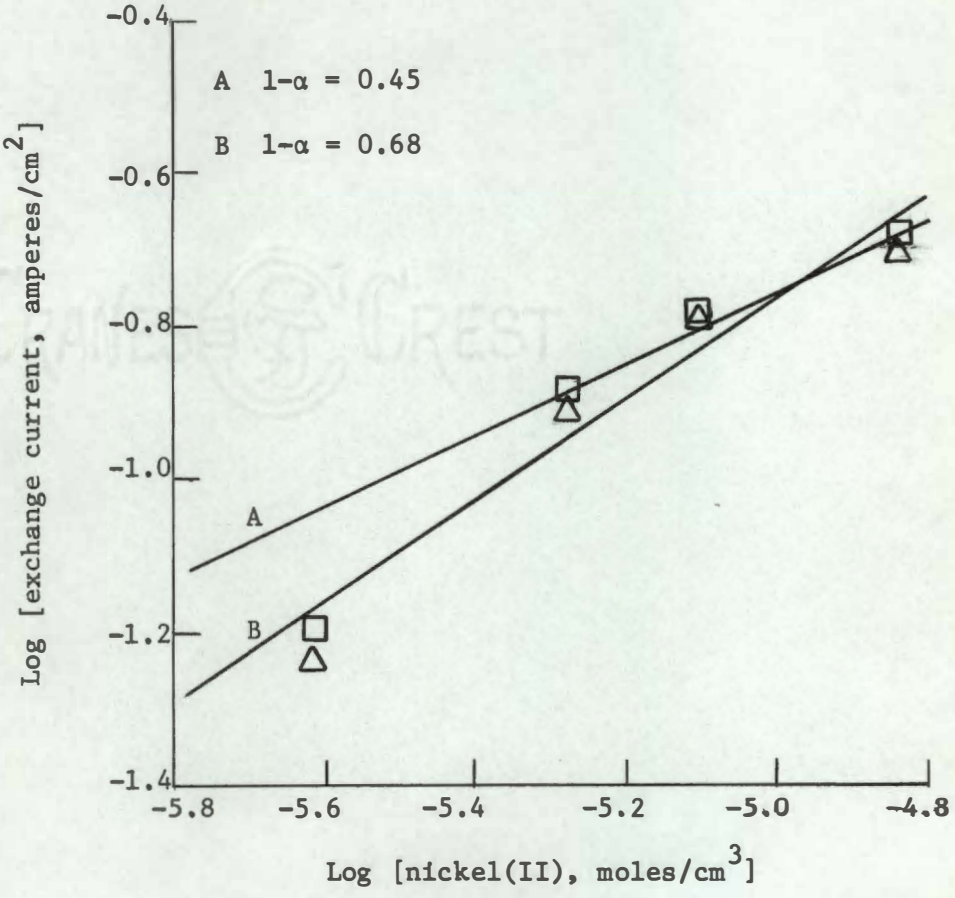

Figure 13. Plot of log [exchange current] versus log [nickel(II)].

TABLE III

SUMMARY OF EXCHANGE CURRENT DENSITY VALUES FOR THE NICKEL(II)/NICKEL COUPLE IN $LiF-BeF_2-ZrF_4$

[Ni(II)], moles/cm^3	Voltage step, mV	$i_{t=0}$, mA	i_0, A/cm^2
2.43×10^{-6}	4.61	0.170	0.064
2.43×10^{-6}	6.10	0.206	0.058
5.26×10^{-6}	4.62	0.309	0.131
5.26×10^{-6}	5.64	0.354	0.122
7.92×10^{-6}	4.58	0.366	0.166
7.92×10^{-6}	5.60	0.442	0.163
1.45×10^{-5}	4.57	0.431	0.209
1.45×10^{-5}	6.14	0.553	0.196

Shapoval and Gorodyskii reported exchange current values on the nickel(II)/nickel couple in a NaCl-KCl melt at 710° which correspond to a rate constant of 1.8×10^{-3} cm/sec.

C. EMF MEASUREMENTS

1. General

The relative standard electrode potentials of several redox couples were determined in the two fluoride solvents from emf measurements on galvanic cells at 500°; these cells consisted of a nickel(II)/nickel reference electrode, containing from $\sim 5 \times 10^{-4}$ to 2×10^{-3} mole fraction nickel(II), and the couple of interest. Since the potential of the reference electrode was shown to include a significant junction potential in some cases, the potential of each reference electrode was related to that of the nickel(II)/nickel couple in the bulk of the melt. Measured potentials were expressed with respect to a hypothetical unit mole fraction nickel(II)/nickel electrode by means of the Nernst equation. The potential of this electrode was arbitrarily set at 0.000 volts.

2. The Beryllium(II)/Beryllium Couple

Since beryllium metal readily reduces zirconium(IV), it was not possible to measure the potential of the beryllium(II)/beryllium couple in $LiF-BeF_2-ZrF_4$. However, this potential was measured in $LiF-BeF_2$ (66-34 mole per cent) by isolating the couple in a boron nitride compartment and measuring the cell emf versus a nickel(II)/nickel electrode in the bulk of a $LiF-BeF_2-ZrF_4$ melt as the nickel(II) concentration was

varied. The results of these measurements are given in Table IV; Figure 14 shows a plot of emf versus log [nickel(II)]. The line drawn through the data points has the theoretical slope, 2.3RT/nF or 0.077 V, given by the Nernst equation. The emf between the beryllium(II)/beryllium electrode and a nickel(II)/nickel reference electrode in another boron nitride compartment was constant at 1.799±0.002 V over an eight day period. In the measurements on the beryllium(II)/beryllium electrode, as in the measurements on the nickel(II)/nickel electrodes contained in boron nitride compartments, the measured emf may have included a significant junction potential across the boron nitride wall. Since in this case there was no way to ascertain the magnitude of the junction potential, it was included in the potential of the electrode couple. A value of -2.120 V was determined with respect to a unit mole fraction nickel(II)/nickel electrode in LiF-BeF_2-ZrF_4 at 500°; the standard state of the beryllium(II) is the solvent composition, LiF-BeF_2 (66-34 mole per cent).

3. The Zirconium(IV)/Zirconium Couple

The potential of a zirconium rod immersed in LiF-BeF_2-ZrF_4 versus a nickel(II)/nickel reference electrode was found to be -1.446±0.01 V over a five day period. This value corrected to a value versus the standard potential of the nickel(II)/nickel couple was -1.549 V. Since Grjotheim[15] found that galvanic cells obeyed the Nernst equation up to about 4.0 mole per cent solutions, it appeared justifiable to extrapolate the potential of the zirconium(IV)/zirconium couple to the hypothetical unit mole fraction solution. This value is -1.742 V.

TABLE IV

SUMMARY OF EMF MEASUREMENTS ON THE NICKEL(II)/NICKEL COUPLE VERSUS A BERYLLIUM(II)/BERYLLIUM ELECTRODE

[Ni(II)], mole fraction	$E_{Ni(II)/Ni}-E_{Be(II)/Be}$, volts
1.54×10^{-4}	1.826
2.47×10^{-4}	1.846
5.01×10^{-4}	1.868
6.41×10^{-4}	1.875
8.95×10^{-4}	1.883
1.10×10^{-3}	1.892

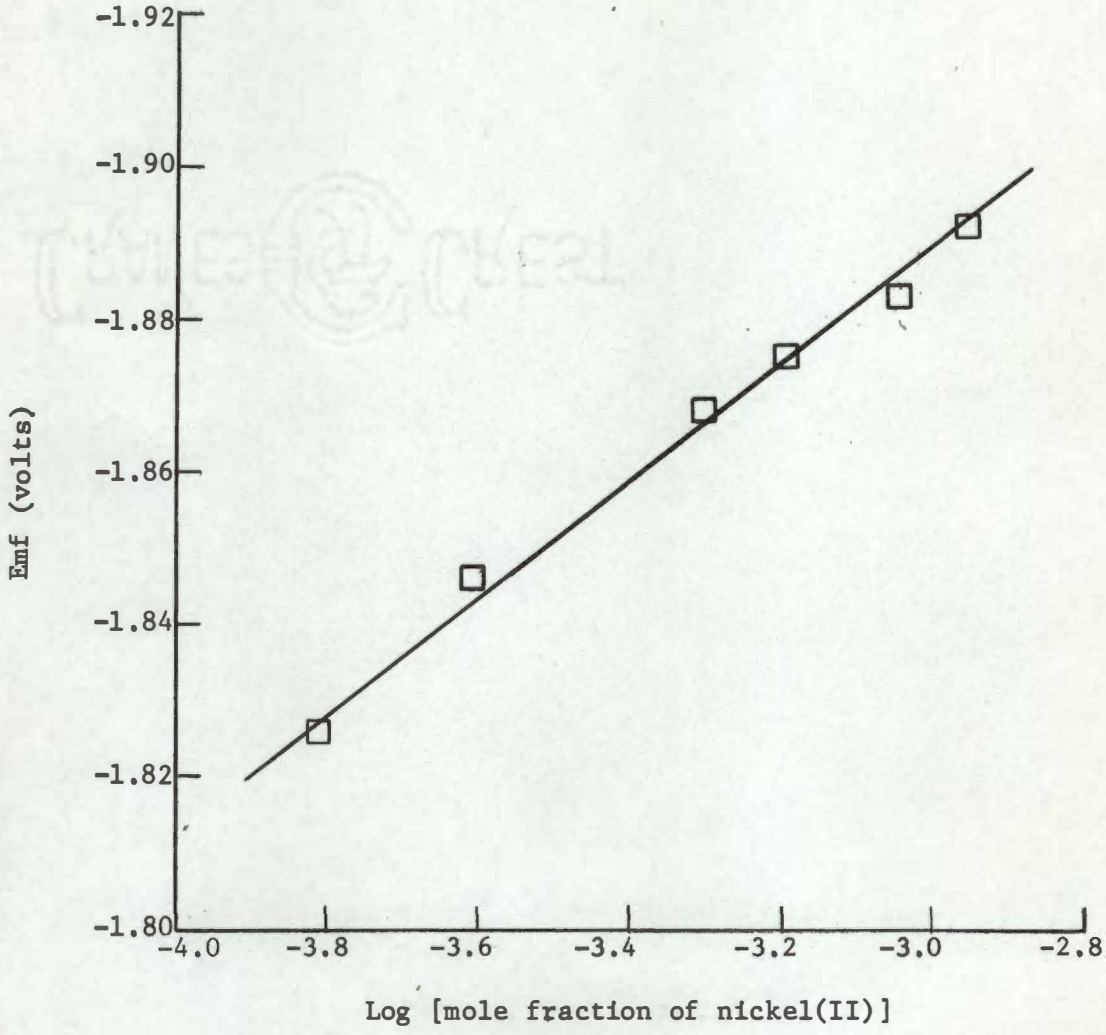

Figure 14. Nernstian plot for the nickel(II)/nickel couple versus a beryllium(II)beryllium electrode in $LiF-BeF_2-ZrF_4$ at 500°.

4. The Uranium(IV)/Uranium(III) Couple

Figure 15 shows a plot of emf measurements, corrected to values versus a unit mole fraction nickel(II)/nickel electrode, versus log [U(IV)/U(III)]. A summary of these values is given in Table V. Measurements were made at total uranium concentrations of 1.4×10^{-3} and 2.6×10^{-3} mole fraction in $LiF-BeF_2-ZrF_4$ at 500°. The line drawn through the data points has the theoretical slope of 0.153 V as given by the Nernst equation. The standard electrode potential determined by extrapolation to a U(IV)/U(III) ratio of unity is -1.480±0.01 V.

5. The Chromium(II)/Chromium Couple

Table VI summarizes emf measurements made in $LiF-BeF_2-ZrF_4$ at 500° on the chromium(II)/chromium couple. Figure 16 shows a plot of corrected emf measurements versus log [chromium(II)]. The line drawn through the data points has the theoretical slope of 0.077 V as given by the Nernst equation. The standard electrode potential determined by extrapolation to a unit mole fraction chromium(II) solution is -0.701±0.01 V.

6. The Chromium(III)/Chromium(II) Couple

Table VII gives a summary of emf measurements on the chromium(III)/chromium(II) couple in $LiF-BeF_2-ZrF_4$ at 500°C. Figure 17 shows a plot of corrected emf measurements versus log [Cr(III)/Cr(II)]. The chromium(III) concentration was varied from 2.7×10^{-4} to 1.3×10^{-3} mole fraction while the chromium(II) concentration was constant at $\sim 1.2 \times 10^{-3}$ mole fraction. The Cr(III)/Cr(II) ratio was determined from voltammetric current-potential

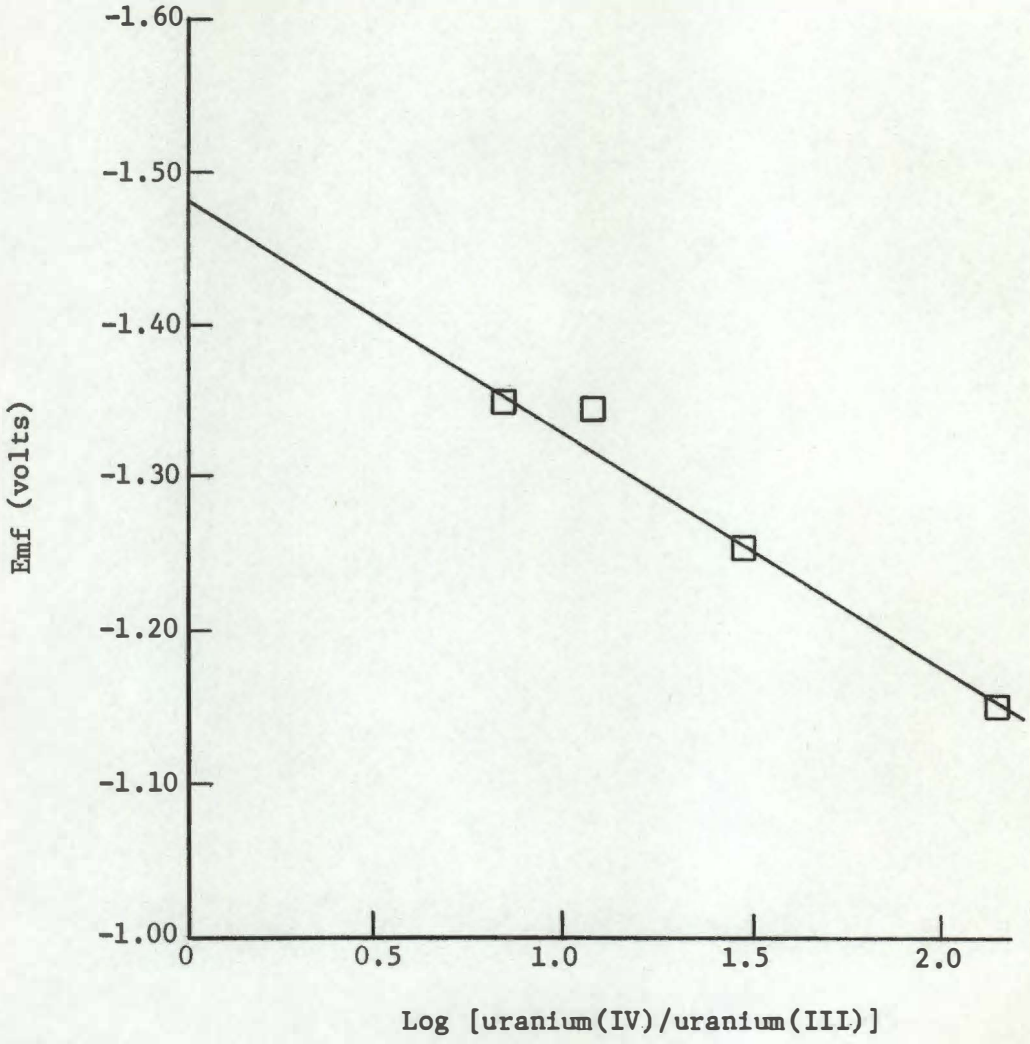

Figure 15. Nernstian plot for the uranium(IV)/ uranium(III) couple in $LiF-BeF_2-ZrF_4$ at 500°.

TABLE V

SUMMARY OF EMF MEASUREMENTS ON THE
URANIUM(IV)/URANIUM(III) COUPLE

$\frac{U(IV)}{U(III)}$ ratio	$E_{ref}-E_{U(IV)/U(III)}$, volts	$E^{\circ}_{Ni(II)/Ni}-E_{U(IV)/U(III)}$ volts
138.0	0.882	1.152
29.4	0.987	1.257
11.8	1.075	1.345
6.7	1.078	1.348

TABLE VI

SUMMARY OF EMF MEASUREMENTS ON THE CHROMIUM(II)/CHROMIUM COUPLE

[Cr(II)], mole fraction	$E_{ref}-E_{Cr(II)/Cr}$, volts	$E^{\circ}_{Ni(II)/Ni}-E_{Cr(II)/Cr}$, volts
7.01×10^{-5}	0.748	1.005
2.29×10^{-4}	0.720	0.977
6.40×10^{-4}	0.694	0.951
1.21×10^{-3}	0.680	0.937

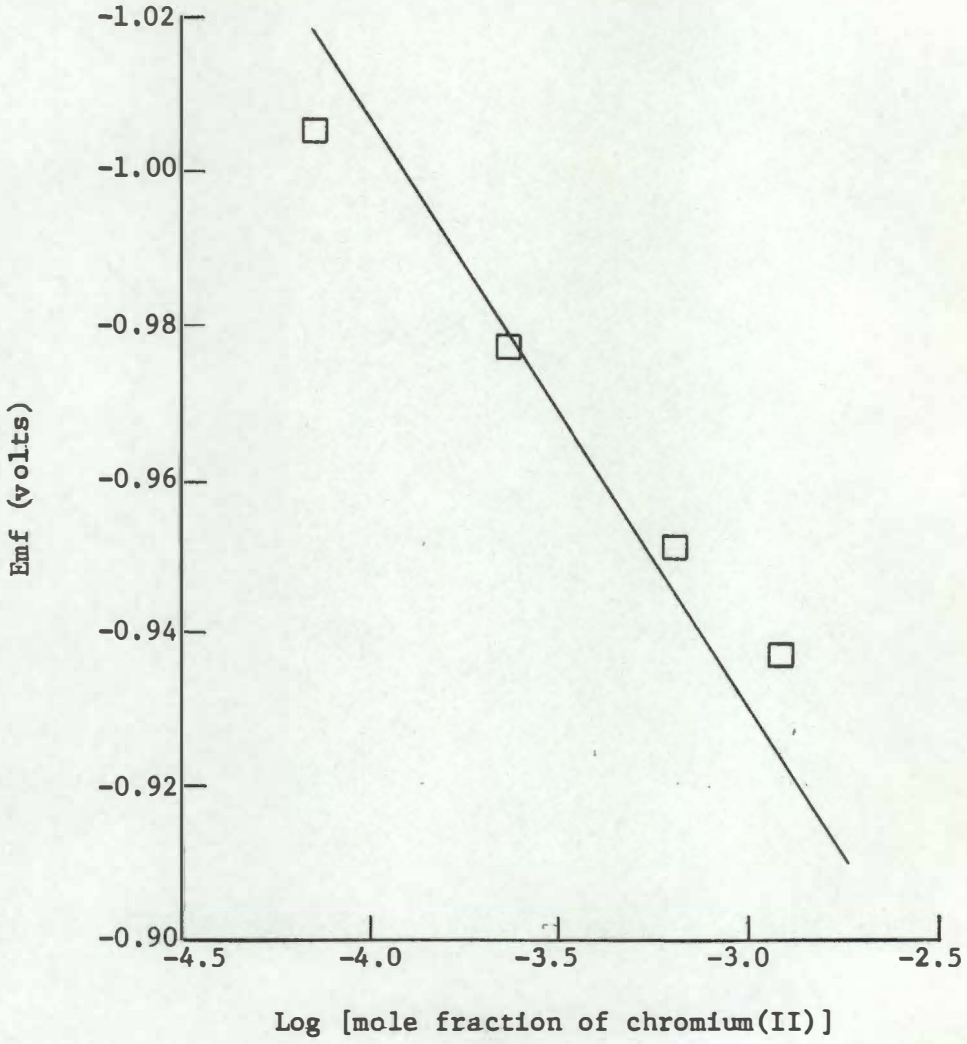

Figure 16. Nernstian plot for the chromium(II)/chromium couple in $LiF-BeF_2ZrF_4$ at 500°.

TABLE VII

SUMMARY OF EMF MEASUREMENTS ON THE CHROMIUM(III)/CHROMIUM(II) COUPLE

$\frac{Cr(III)}{Cr(II)}$ ratio	$E_{ref}-E_{Cr(III)/Cr(II)}$, volts	$E^{\circ}_{Ni(II)/Ni}-E_{Cr(III)/Cr(II)}$, volts
0.24	0.360	0.617
0.35	0.320	0.577
0.52	0.295	0.552
0.78	0.270	0.527
1.15	0.253	0.510

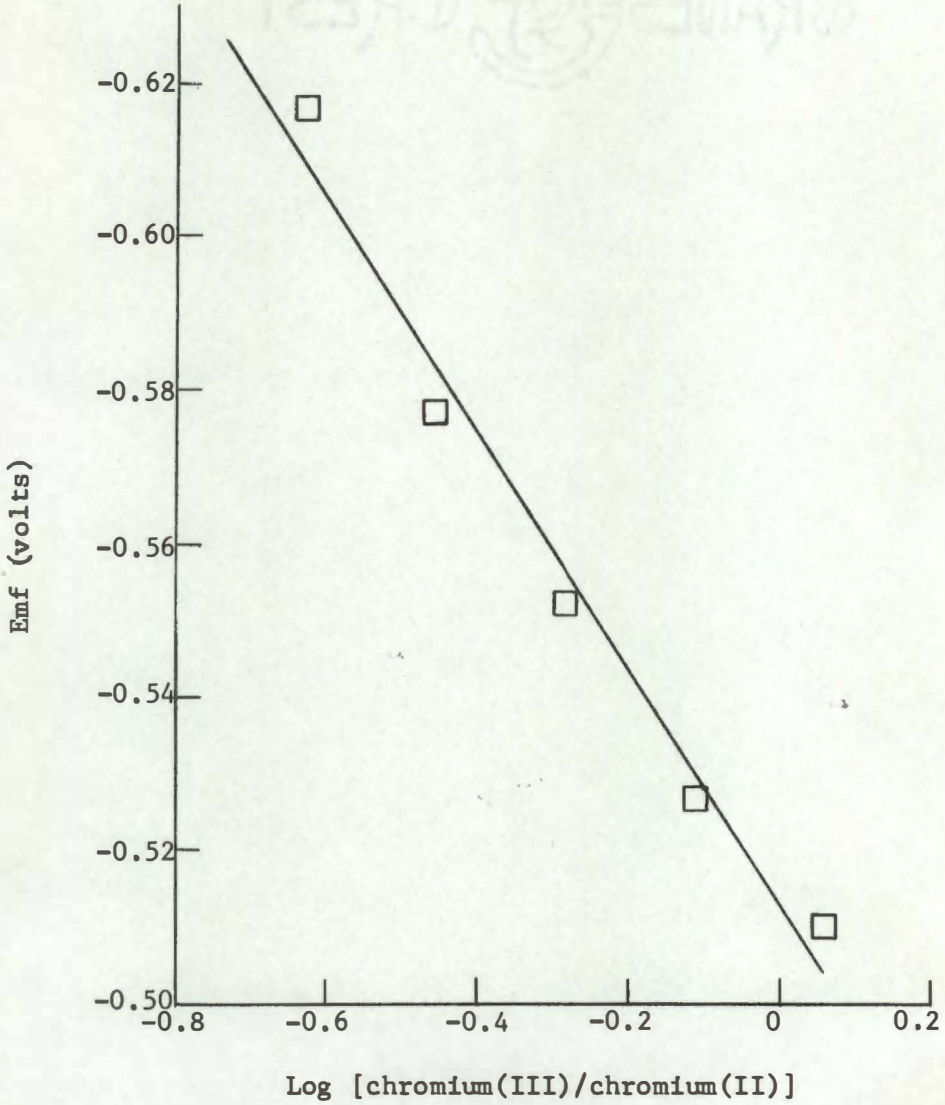

Figure 17. Nernstian plot for the chromium(III)/chromium(II) couple in LiF-BeF_2-ZrF_4 at 500°.

curves obtained by scanning both cathodically and anodically from the equilibrium potential of the chromium(III)/chromium(II) couple. The peak current in the cathodic direction is proportional to the chromium(III) concentration while the peak current in the anodic direction is proportional to the chromium(II) concentration. The ratio of peak currents is equal to the Cr(III)/Cr(II) ratio. The line drawn through the data points in Figure 17 has the theoretical slope of 0.153 V as given by the Nernst equation. The standard electrode potential determined at a Cr(III)/Cr(II) ratio of unity is -0.514±0.01 V.

7. The Iron(II)/Iron Couple

Figure 18 shows a plot of corrected emf measurements made in LiF-BeF_2-ZrF_4 at 500° versus log [iron(II)]. These measurements are summarized in Table VIII. The line drawn through the data points has the theoretical slope of 0.077 V as given by the Nernst equation. The standard electrode potential determined by extrapolation to a unit mole fraction solution of iron(II) is -0.410±0.01 V.

Figure 19 shows a plot of corrected emf measurements made in LiF-NaF-KF at 500° versus log [iron(II)]. These measurements are summarized in Table VIII. The line drawn through the data points has the theoretical slope of 0.077 V as given by the Nernst equation. The standard electrode potential determined by extrapolation to a unit mole fraction iron(II) solution is -0.390±0.01 V.

8. The Iron(III)/Iron(II) Couple

Figure 20 shows a plot of corrected emf measurements made in LiF-BeF_2-ZrF_4 at 500° versus log [Fe(III)/Fe(II)]. These measurements are

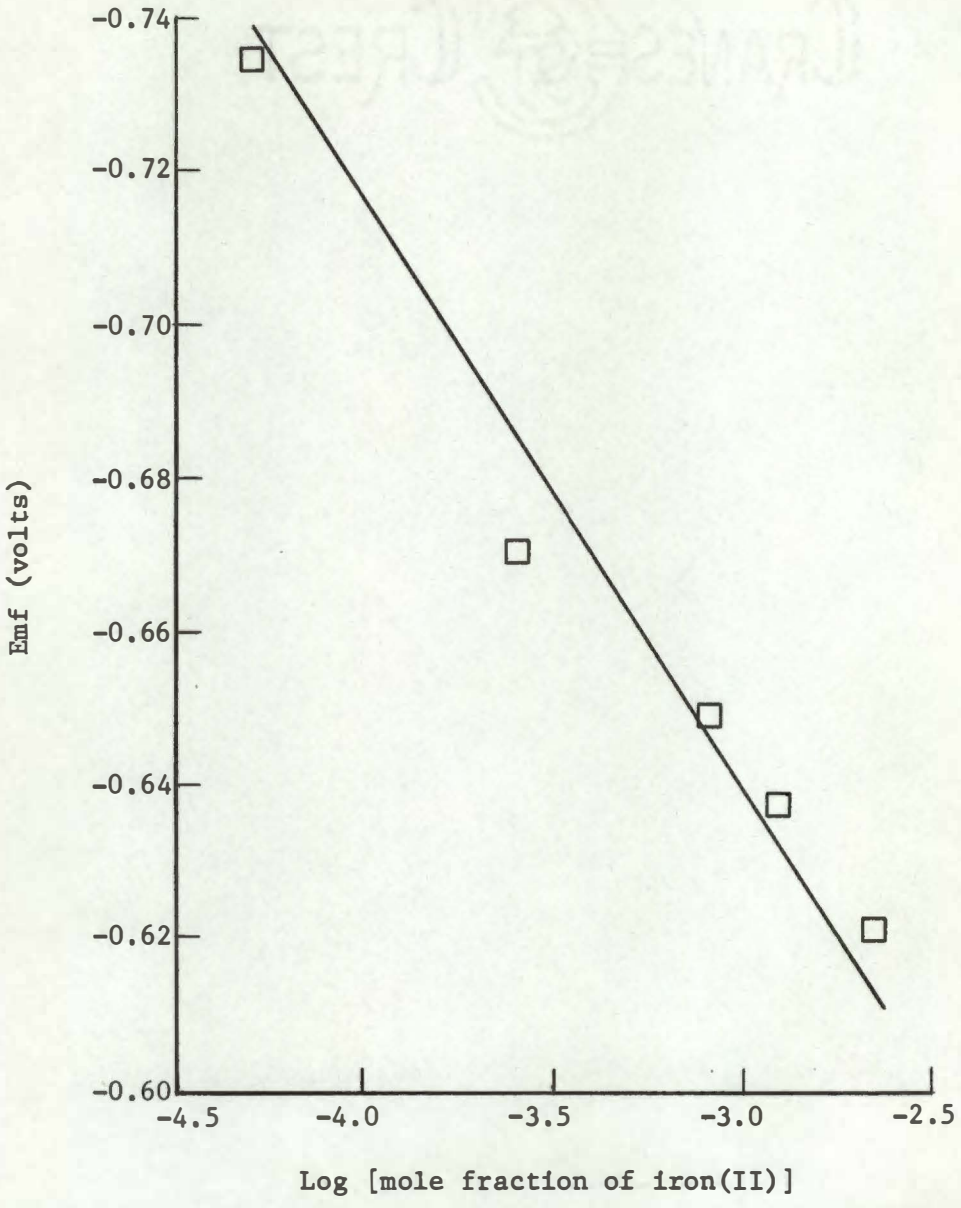

Figure 18. Nernstian plot for the iron(II)/iron couple in LiF-BeF_2-ZrF_4 at 500°.

TABLE VIII

SUMMARY OF EMF MEASUREMENTS ON THE IRON(II)/IRON COUPLE

[Fe(II)], mole fraction	$E_{ref}-E_{Fe(II)/Fe}$, volts	$E^{\circ}_{Ni(II)/Ni}-E_{Fe(II)/Fe}$, volts
4.98×10^{-5}[a]	0.415	0.734
2.53×10^{-4}[a]	0.351	0.670
8.22×10^{-4}[a]	0.330	0.649
1.24×10^{-3}[a]	0.318	0.637
2.22×10^{-3}[a]	0.302	0.621
1.92×10^{-5}[b]	0.526	0.744
8.64×10^{-5}[b]	0.491	0.709
1.69×10^{-4}[b]	0.446	0.664
3.46×10^{-4}[b]	0.431	0.649
6.64×10^{-4}[b]	0.419	0.637

[a] In $LiF-BeF_2-ZrF_4$.

[b] In LiF-NaF-KF.

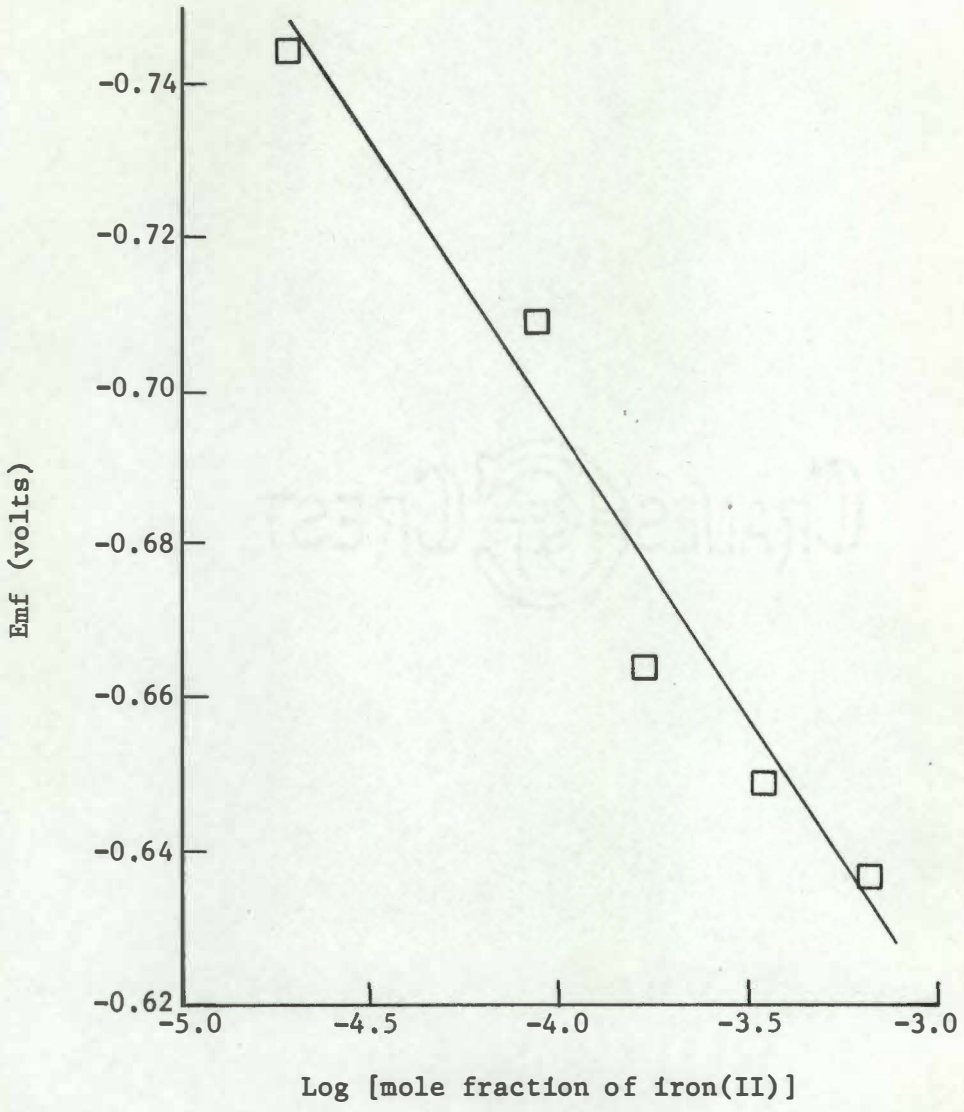

Figure 19. Nernstian plot for the iron(II)/iron couple in LiF-NaF-KF at 500°.

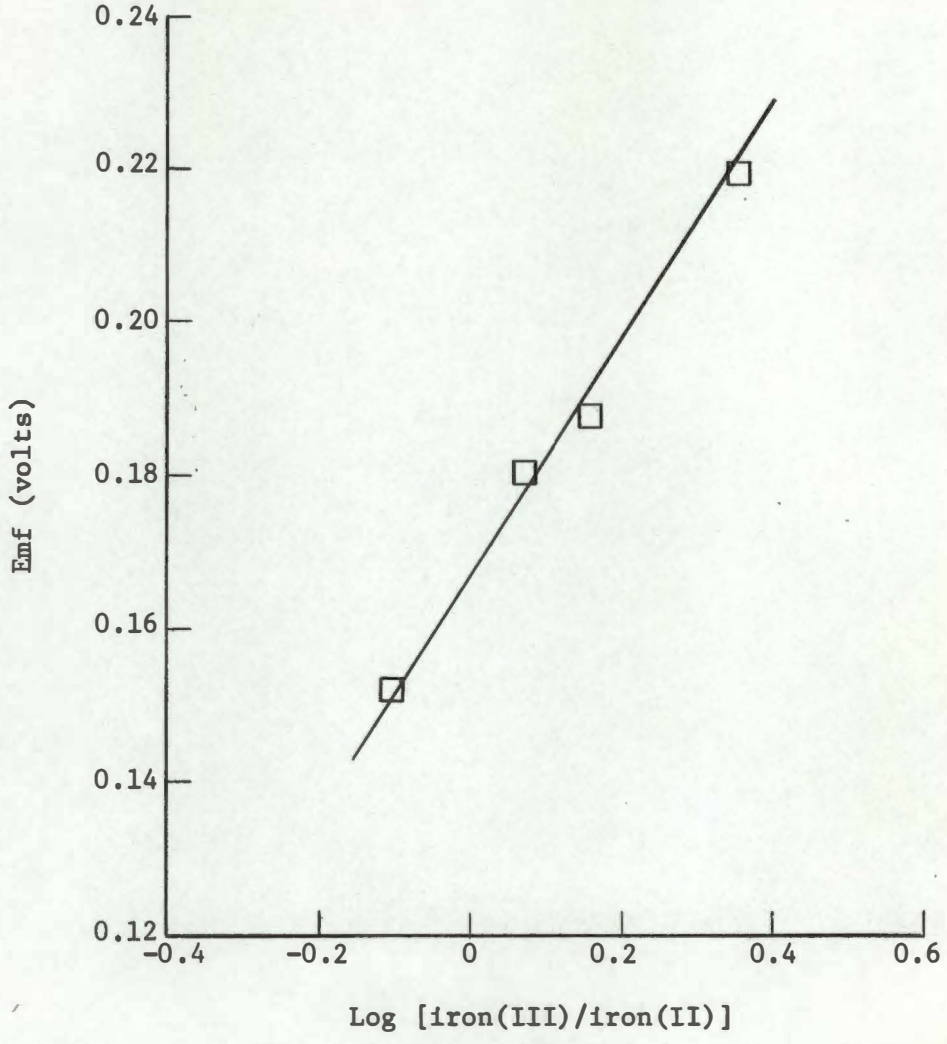

Figure 20. Nernstian plot for the iron(III)/iron(II) couple in $LiF-BeF_2-ZrF_4$ at 500°.

summarized in Table IX. The iron(III) concentration was varied from 7.0×10^{-5} to 4×10^{-4} mole fraction while the iron(II) concentration was varied from 5.9×10^{-5} to 2.8×10^{-4} mole fraction. The line drawn through the data points has the theoretical slope of 0.153 V as given by the Nernst equation. The standard electrode potential determined at a Fe(III)/Fe(II) ratio of unity is 0.166±0.01 V.

Figure 21 shows a plot of corrected emf measurements made in LiF-NaF-KF at 500° versus log [Fe(III)/Fe(II)]. A summary of these measurements is given in Table IX. The iron(III) concentration was varied from 2.5×10^{-4} to 5.2×10^{-4} mole fraction while the iron(II) concentration was varied from 1.6×10^{-4} to 5.6×10^{-4} mole fraction. The line drawn through the data points has a theoretical slope of 0.153 V as given by the Nernst equation. The standard electrode potential determined at a Fe(III)/Fe(II) ratio of unity is -0.200±0.01 V.

9. Summary of Electrode Potentials

Table X summarizes the standard electrode potentials determined in this investigation. The values determined in LiF-BeF_2-ZrF_4 agree rather well with values calculated by Baes,[19] column IV of Table I, page 6, for a LiF-BeF_2 (66-34 mole per cent) melt. It would be expected that the properties of these two melts would be rather similar. In all instances, the values determined in this study were lower than the values calculated by Baes. The 100 mV difference observed between the two values for the beryllium(II)/beryllium couple could be partially or totally due to the inclusion of a junction potential in the value

TABLE IX

SUMMARY OF EMF MEASUREMENTS ON THE IRON(III)/IRON(II) COUPLE

$\frac{Fe(III)}{Fe(II)}$ ratio	$E_{ref}-E_{Fe(III)/Fe(II)}$, volts	$E^{\circ}_{Ni(II)/Ni}-E_{Fe(III)/Fe(II)}$, volts
0.79[a]	-0.428	-0.152
1.18[a]	-0.456	-0.180
1.44[a]	-0.463	-0.187
2.29[a]	-0.495	-0.219
0.43[b]	0.042	0.260
0.60[b]	0.016	0.234
0.86[b]	-0.014	0.204
1.35[b]	-0.040	0.178
2.50[b]	-0.068	0.150

[a]In $LiF-BeF_2-ZrF_4$.

[b]In LiF-NaF-KF.

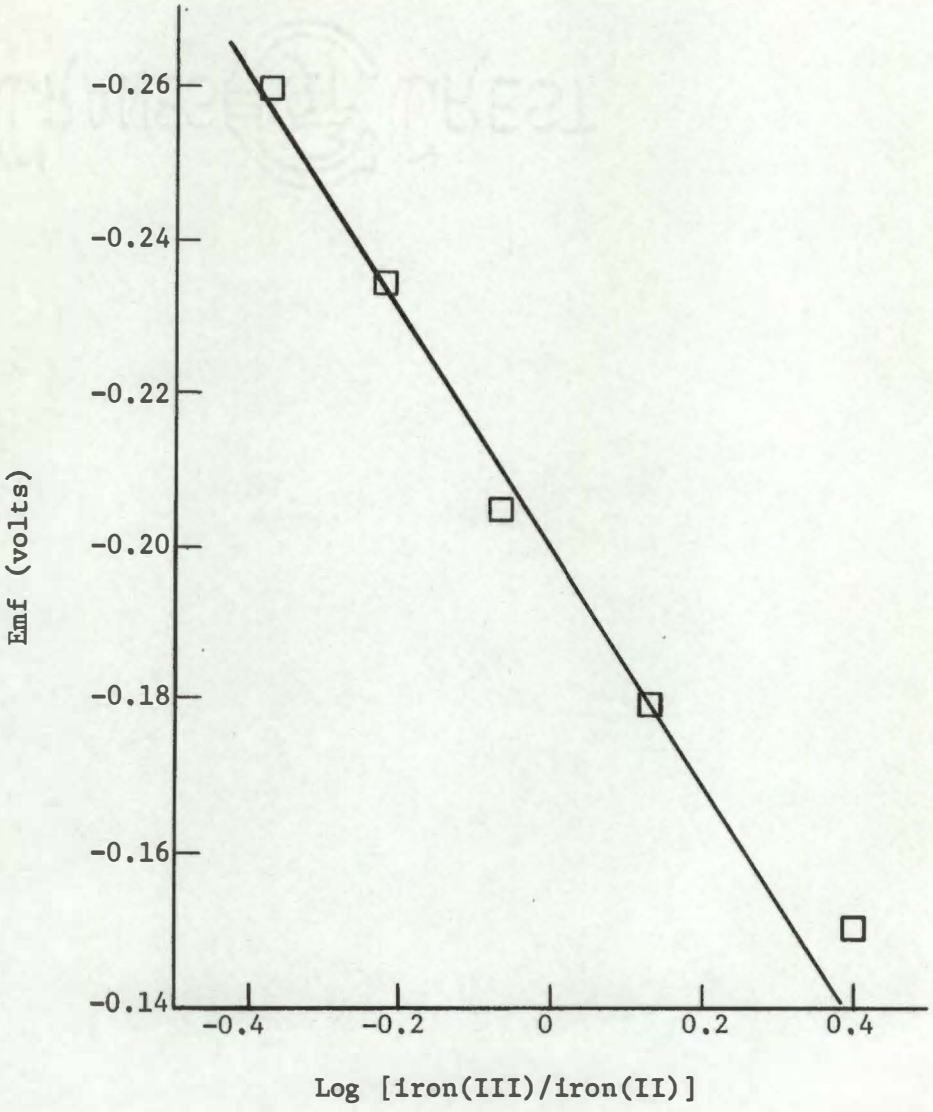

Figure 21. Nernstian plot for the iron(III)/iron(II) couple in LiF-NaF-KF at 500°.

TABLE X

MEASURED ELECTRODE POTENTIALS IN MOLTEN FLUORIDES

Electrode couple	Standard Electrode Potentials,[a] volts In $LiF-BeF_2-ZrF_4$ at 500°	In LiF-NaF-KF at 500°
Be(II)/Be	-2.120	
Zr(IV)/Zr	-1.742	
U(IV)/U(III)	-1.480	
Cr(II)/Cr	-0.701	
Cr(III)/Cr(II)	-0.514	
Fe(II)/Fe	-0.410	-0.390
Ni(II)/Ni	0.000	0.000
Fe(III)/Fe(II)	0.166	-0.200

[a]Standard state for all solutes except beryllium(II) is the hypothetical unit mole fraction solution. The beryllium(II) standard state is the solvent composition, $LiF-BeF_2$ (66-34 mole per cent).

determined in this study. The other differences observed between the values reported by Baes and those measured in this study range from 3 mV (for the iron(II)/iron couple) to 88 mV (for the chromium(II)/chromium couple). These differences are difficult to explain at this time solely on the basis of differences in solvent composition.

The values determined in LiF-NaF-KF do not agree well with the values estimated by chronopotentiometry at 750° by Mellors and Senderoff,[17] column II of Table I, page 6; however, it is impossible to make a valid comparison between the two sets of data without knowing the temperature coefficients for the galvanic cells involved. Manning[42,43] has given voltammetric current-potential curves for the iron(II)/iron, iron(III)/iron(II) and nickel(II)/nickel couples in LiF-NaF-KF at ∿ 500°. However, it is impossible to compare the relative oxidation-reduction potentials observed in these current-potential curves since a quasi-reference electrode was employed in the measurements. This electrode is poised by the potential of the melt which is dependent on the species in the melt; its potential varies somewhat between melts. Also, the potential of the reduction wave of a metal ion to a metal is dependent on the metal ion concentration.

A comparison between the redox couples determined in both solvents indicates that the change in solvents has little effect on the relative difference in electrode potentials of the nickel(II)/nickel and iron(II)/iron couples, 0.390 V in LiF-NaF-KF and 0.410 V in LiF-BeF_2-ZrF_4. However, this is not the case for the iron(III)/iron(II) couple; the relative difference in electrode potentials of the iron(III)/iron(II) and

the iron(II)/iron couples is 0.190 V in LiF-NaF-KF while it is 0.576 V in LiF-BeF_2-ZrF_4. Thus, iron(III) is 0.386 V or 8.8 kcal more stable relative to iron(II) in LiF-NaF-KF than in LiF-BeF_2-ZrF_4.

D. VOLTAMMETRIC DETERMINATION OF HIGH U(IV)/U(III) RATIOS

1. Considerations

Simultaneous with the determination of the standard electrode potential of the uranium(IV)/uranium(III) couple, a simple voltammetric method was developed for the determination of the U(IV)/U(III) ratio where the uranium(IV) concentration is much greater than the uranium(III) concentration (approximately ten or greater). This method involves the measurement of the equilibrium potential of the melt, measured with an inert electrode immersed in the melt, with respect to the voltammetric equivalent of the standard electrode potential, the polarographic $E_{1/2}$. From this measurement, the ratio is readily calculated from equation (1), page 11:

$$E_{eq}-E_{1/2} = \frac{2.3RT}{nF} \log \frac{U(IV)}{U(III)}$$

This method should be applicable to the uranium(IV)/uranium(III) couple since Mamantov and Manning[44] have shown the couple to be reversible in LiF-BeF_2-ZrF_4.

2. Results

Figure 22 shows a voltammetric current-potential curve obtained in LiF-BeF_2-ZrF_4 at 500° by initially scanning cathodically from zero

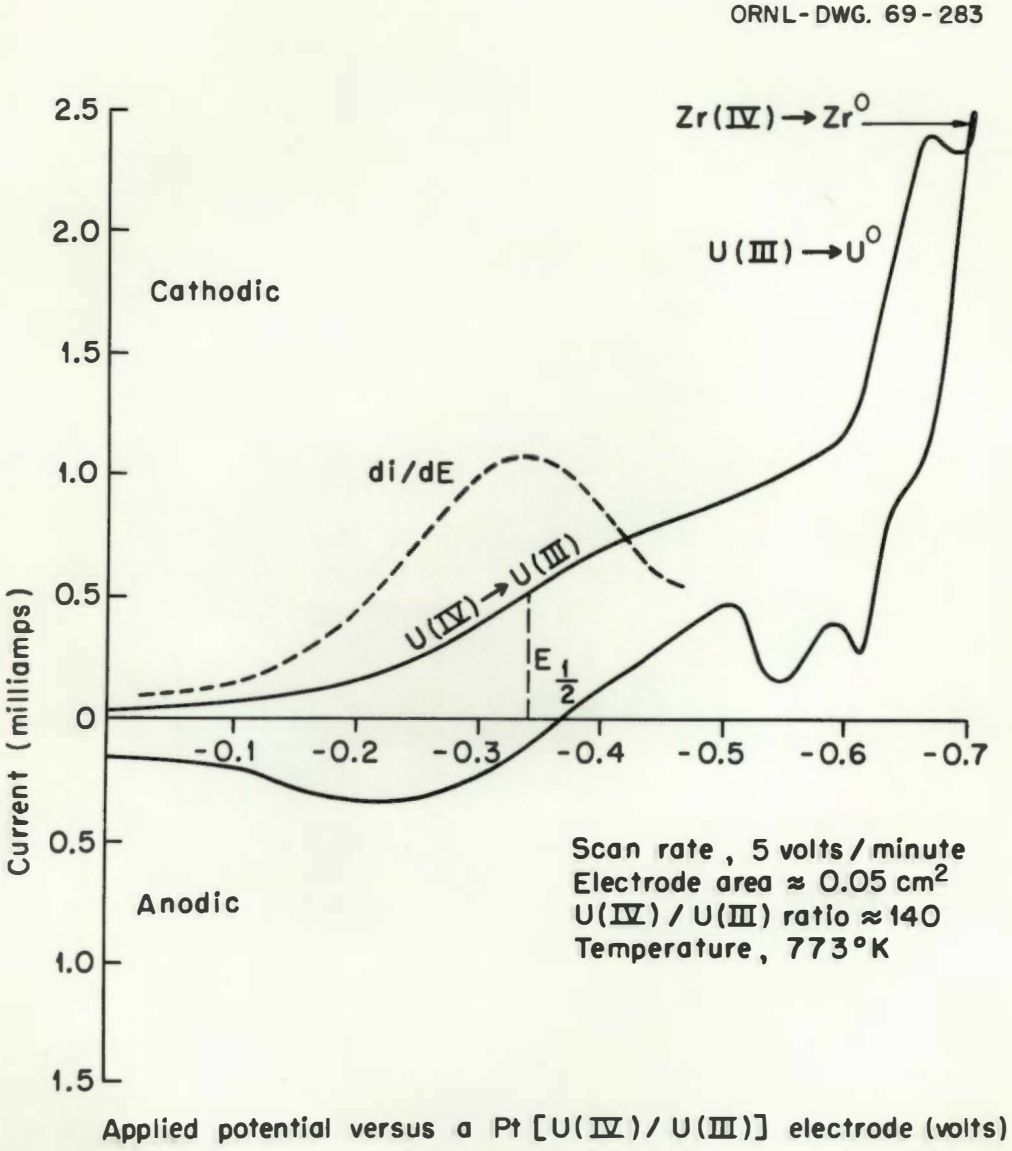

Figure 22. Voltammogram for the reduction of uranium(IV) in $LiF-BeF_2-ZrF_4$ at 500°.

volts and reversing the direction of scan at the reduction potential of zirconium(IV). The total uranium concentration was 2.6×10^{-3} mole fraction with a uranium(IV)/uranium(III) ratio of approximately 140. Since a well-defined wave for the reaction U(IV) + e = U(III) was not observed under the experimental conditions, a derivative of the current-potential curve (Figure 22, the dashed line) was obtained. The peak of the derivative curve was taken as an approximation of $E_{1/2}$. Table XI gives a comparison between U(IV)/U(III) ratios determined by this method and those determined from spectrophotometric analysis by Dr. J. P. Young.

It is interesting to note that in Figure 22 a wave is seen for the reduction of uranium(III) to uranium metal on the nickel working electrode. No such wave was observed on a platinum working electrode while the position of the zirconium(IV) reduction wave was the same for both working electrodes. Mamantov and Manning[44] did not observe such a wave on a platinum working electrode either. It seems that the formation of a nickel-uranium alloy is responsible for the uranium(III) reduction at a nickel working electrode.

3. Discussion

The agreement obtained between the two independent methods of analysis was very good considering the instability of uranium(III) in the experimental system; uranium(III) could not be maintained for more than 24 hours. This was apparently due to the diffusion of oxygen, which readily oxidizes uranium(III) to uranium(IV), through the dry box gloves.

The advantages of this method are

(i) an isolated reference electrode is not required

TABLE XI

THE DETERMINATION OF THE U(IV)/U(III) RATIO

Voltammetry		Spectrophotometry	
ΔE,[a] volts	U(IV)/U(III) ratio[b]	ΔE,[b] volts	U(IV)/U(III) ratio[a]
0.345	180	0.328	138
0.225	29.6	0.225	29.4
0.153	10.0	0.164	11.8
0.130	7.1	0.135	6.7

[a]Measured values.

[b]Calculated values.

(ii) no independent knowledge of the relative standard electrode potentials is required

(iii) the electrode area need not be known.

The method is applicable to the determination of ratios of any redox couple where both species are soluble and the electrode reaction is reversible. A stationary working electrode was employed in this study, but the method should also be applicable to the rotating disk and dropping mercury working electrodes. The method in its present form is only useful for high ratios of Ox/Red (or vice versa) since the diffusion or limiting current for one species is assumed to be essentially negligible compared to that of the other species. This method should also be useful in other non-aqueous solvents where reference electrodes and electrode potential data are not available.

CHAPTER IV

SUMMARY

The utility of a nickel(II)/nickel reference electrode contained in a boron nitride compartment was investigated in molten LiF-BeF_2-ZrF_4 (65.6-29.4-5.0 mole per cent) and LiF-NaF-KF (46.5-11.5-42.0 mole per cent) by making emf measurements on nickel(II)/nickel concentration cells. The nickel(II)/nickel couple was shown to obey the Nernst equation. It was found that the reference electrode in some cases had a significant junction potential across the boron nitride wall; even with this unpredictable junction potential, the potential of such electrodes appeared reasonably stable for periods of at least two weeks. Thus, such a reference electrode can be utilized for making emf measurements in molten fluoride solvents by relating its potential to a common point for each set of emf measurements.

The kinetics of the charge transfer reaction Ni(II) + 2e = Ni were investigated employing the voltage-step method. Apparent adsorption of nickel(II) at the microelectrode surface prevented a quantitative determination of the kinetic parameters; however, application of the simple theory to the data yielded a range in the transfer coefficient α of 0.32 to 0.55. The corresponding range in the heterogeneous standard rate constant k^o was 1.6×10^{-4} to 2.3×10^{-3} cm/sec.

Standard electrode potentials of several redox couples were determined in molten fluorides. Emf measurements on galvanic cells were made employing nickel(II)/nickel reference electrodes isolated in boron

nitride compartments. Standard electrode potentials were determined by relating the potential of each reference electrode to the standard electrode potential of the nickel(II)/nickel couple (arbitrarily set at 0.000 V). This was accomplished by measuring the potential of the reference electrode with respect to a nickel(II)/nickel electrode in the bulk of the melt. The following values were determined in $LiF-BeF_2-ZrF_4$ at 500°: beryllium(II)/beryllium, -2.120 V; zirconium(IV)/zirconium, -1.742 V; uranium(IV)/uranium(III), -1.480V; chromium(II)/chromium, -0.701 V; chromium(III)/chromium(II), -0.514 V; iron(II)/iron, -0.410 V; nickel(II)/nickel, 0.000 V; iron(III)/iron(II), 0.166 V. The following values were determined in LiF-NaF-KF at 500°: iron(II)/iron, -0.390 V; iron(III)/iron II, -0.200 V; nickel(II)/nickel, 0.000 V.

A simple voltammetric method was developed for the determination of high U(IV)/U(III) ratios. The method involves the measurement of the equilibrium potential of the melt with respect to the voltammetric equivalent of the standard electrode potential, the polarographic $E_{1/2}$, of the uranium(IV)/uranium(III) couple. Good agreement was obtained between this method and spectrophotometric analysis of molten salt samples.

BIBLIOGRAPHY

BIBLIOGRAPHY

1. Yu. K. Delimarskii and B. F. Markov, "The Electrochemistry of Fused Salts," Sigma Press, Washington, D. C., 1961.

2. G. J. Janz, "Molten Salt Handbook," Academic Press, New York, N. Y., 1967, pp. 265-286.

3. R. Laity in "Reference Electrodes," D. J. G. Ives and G. J. Janz, Eds., Academic Press, New York, N. Y., 1961, pp. 524-606.

4. H. A. Laitinen and C. H. Liu, J. Am. Chem. Soc., 80, 1015 (1958).

5. A. F. Alabyshev, M. F. Lantratov and A. G. Morachveskii, "Reference Electrodes for Fused Salts," Sigma Press, Washington, D. C., 1965.

6. H. A. Laitinen and J. W. Pankey, J. Am. Chem. Soc., 81, 1053 (1959).

7. J. Simons and J. H. Hildebrand, J. Am. Chem. Soc., 46, 2223 (1924).

8. A. J. Arvia and J. B. de Cusminsky, J. Chem. Phys., 36, 1089 (1962).

9. A. J. Arvia and J. B. de Cusminsky, Trans. Far. Soc., 58, 1019 (1962).

10. G. Dirian, K. A. Romberger and C. F. Baes, Jr., U.S.A.E.C. Report ORNL-3789, 76 (1965).

11. B. F. Hitch and C. F. Baes, Jr., U.S.A.E.C. Report ORNL-4257 (1968).

12. H. Coriou, J. Dirian and J. Hure, J. Chim. Phys., 52, 479 (1955).

13. R. Winand and G. Chaudron, Comptes rendus, 264c, 649 (1967).

14. S. Pizzini and R. Morlotti, Electrochim. Acta., 10, 1033 (1965).

15. K. Grjotheim, Z. Physik. Chem., N. F., 11, 150 (1957).

16. S. Senderoff, G. W. Mellors and W. J. Reinhart, J. Electrochem. Soc., 112, 840 (1965).

17. G. W. Mellors and S. Senderoff in "Applications of Fundamental Thermodynamics to Metallurgical Processes," G. R. Fitterer, Ed., Gordon and Breach, New York, N. Y., 1967, pp. 81-103.

18. Yu. K. Delimarskii and F. F. Grigorenko, Ukr. Khim. Zh., 22, 726 (1956).

19. C. F. Baes, Jr. in SM-66/60, "Thermodynamics," Vol. I, IAEA, Vienna, 1966.

20. D. M. Moulton, W. P. Teichert, W. K. R. Finnell, W. R. Grimes and J. H. Shaffer, U.S.A.E.C. Report ORNL-4229, 39 (1968).

21. W. J. Hamer, M. S. Malmberg and B. Rubin, J. Electrochem. Soc., 112, 750 (1965).

22. A. D. Graves, G. J. Hills and D. Inman in "Advances in Electrochemistry and Electrochemical Engineering," Vol. 4, P. Delahay, Ed., Interscience, New York, N. Y., 1966, pp. 117-183.

23. H. A. Laitinen and R. A. Osteryoung in "Fused Salts," B. R. Sundheim, Ed., McGraw-Hill, New York, N. Y., 1964, pp. 264-282.

24. J. E. B. Randles and W. White, Z. Electrochem., 59, 666 (1955).

25. H. A. Laitinen, R. P. Tischer and D. K. Roe, J. Electrochem. Soc., 107, 546 (1960).

26. Yu. K. Delimarskii, V. I. Shapoval and A. V. Gorodyskii, Ukr. Khim., Zh., 30, 677 (1964).

27. B. J. Sturm and R. E. Thoma, U.S.A.E.C. Report ORNL-3789, 83 (1965).

28. W. D. Powers, S. I. Cohen and N. D. Greene, Nucl. Sci. Eng., 71, 200 (1963).

29. K. Grjotheim and G. M. Rosenblatt in "Selected Topics in High-Temperature Chemistry," T. Forland, K. Grjotheim, K. Motzfeldt and S. Urnes, Eds., Universitetsforlaget, Oslo, 1966, pp. 117-183.

30. W. Vielstich and P. Delahay, J. Am. Chem. Soc., 79, 1874 (1957).

31. H. Gerischer and W. Vielstich, Z. Physik. Chem., N. F., 3, 16 (1955).

32. K. B. Oldham and R. A. Osteryoung, J. Electroanal. Chem., 11, 397 (1966).

33. P. Delahay, "New Instrumental Methods in Electrochemistry," Interscience, New York, N. Y., 1954, pp. 38, 119.

34. R. S. Nicholson and I. Shain, Anal. Chem., 36, 706 (1964).

35. W. R. Grimes, D. R. Cuneo, F. F. Blankenship, G. W. Keilhotz, H. F. Poppendiek and M. T. Robinson in "Fluid Fuel Reactors," J. A. Lane, H. G. MacPherson and F. Moslan, Eds., Addison-Wesley, Reading, Mass., 1958, p. 584.

36. D. J. Fischer, M. T. Kelley, W. L. Maddox, and R. W. Stelzner, U.S.A.E.C. Report ORNL-3537, 16 (1963).

37. J. P. Young, Inorg. Chem., 6, 1486 (1967).

38. K. M. Taylor, Ind. Eng. Chem., 47, 2506 (1955).

39. B. Timmer, M. Sluyters-Rehbach and J. H. Sluyters, J. Electroanal. Chem., 15, 343 (1967).

40. F. C. Anson, Ann. Rev. Phys. Chem., 19, 83 (1968).

41. H. Matsuda and P. Delahay, Coll. Czech. Chem. Communs., 25, 2977 (1960).

42. D. L. Manning, J. Electroanal. Chem., 6, 227 (1963).

43. D. L. Manning, J. Electroanal. Chem., 7, 302 (1964).

44. G. Mamantov and D. L. Manning, Anal. Chem., 38, 1494 (1966).

VITA

The author, born March 16, 1942 in Charleston, S. C., is the son of Mr. and Mrs. Howard W. Jenkins of Madison, Tennessee. Primary and secondary education was obtained in the Nashville-Davidson County school system with graduation from Du Pont High School in June 1960. The author received a B.S. degree in Chemistry from Tennessee Technological University in June 1964. He entered the Graduate School of the University of Tennessee in September 1964.

The author married Doris Kathleen Avril on August 28, 1965. While attending the University of Tennessee, the author held a teaching assistantship, an A.E.C. research assistantship and an Oak Ridge Graduate Fellowship.